

1 **Gut microbiome composition and function – including**
2 **transposase gene abundance - varies with age, but not**
3 **senescence, in a wild vertebrate**

4
5 **Wild gut microbiome changes with age**

6
7 Chuen Zhang Lee^{1*}, Sarah F. Worsley¹, Charli S. Davies¹, Ece Silan², Terry Burke³,
8 Jan Komdeur⁴, Falk Hildebrand², Hannah L. Dugdale⁴, David S. Richardson^{1,5*}

9
10
11 ¹ School of Biological Sciences, University of East Anglia, Norfolk, UK

12 ² Quadram Institute, Norwich Research Park, Norfolk, UK

13 ³ Ecology and Evolutionary Biology, School of Biosciences, University of Sheffield,
14 Sheffield, UK

15 ⁴ Groningen Institute for Evolutionary Life Sciences (GELIFES), University of Groningen,
16 Groningen, The Netherlands

17 ⁵ Nature Seychelles, Roche Caiman, Mahé, Republic of Seychelles

18
19 *Correspondence: david.richardson@uea.ac.uk, chuen.lee@uea.ac.uk

20
21
22 **Study funding**

23 CZL was funded by the UK Biotechnology and Biological Sciences Research Council
24 (BBSRC) Norwich Research Park Biosciences Doctoral Training Partnership (Grant number
25 BB/T008717/1). DSR and HLD were funded by a Natural Environment Research Council
26 (NERC) grant (NE/S010939/1). SFW was funded by a Leverhulme Trust Early Career
27 Fellowship (ECF-2023-433). CSD was funded by the NERC EnvEast Doctoral Training
28 Programme grant NE/L002582/1). FH and ES were supported by the European Research
29 Council H2020 StG (erc-stg-948219, EPYC). FH was also supported by BBSRC Institute
30 Strategic Programme Food Microbiome and Health (BB/X011054/1, BBS/E/
31 F/000PR13631), Earlham Institute ISP Decoding Biodiversity BBX011089/1,
32 (BBS/E/ER/230002A and BBS/E/ER/230002B). JK and DSR were funded by Dutch
33 Science Council grant (ALW NWO Grant No. ALWOP.531), JK was funded by NWO TOP
34 grant 854.11.003 and NWO VICI 823.01.014 also from Dutch science council.

37 **Abstract**

38 Studies on wild animals, mostly undertaken using 16S metabarcoding, have yielded
39 ambiguous evidence regarding changes in the gut microbiome (GM) with age and
40 senescence. Furthermore, variation in GM function has rarely been studied in such wild
41 populations, despite GM metabolic characteristics potentially being associated with host
42 senescent declines. Here, we used seven years of longitudinal sampling and shotgun
43 metagenomic sequencing to investigate taxonomic and functional changes in the GM of
44 Seychelles warblers (*Acrocephalus sechellensis*) with age and senescence. Our results
45 suggest that taxonomic GM species richness declines with age and in the terminal year,
46 with this terminal decline occurring consistently across all ages. Taxonomic and functional
47 GM composition also shifted with host age. However, all the changes we identified
48 occurred linearly with adult age, with little evidence of accelerated change in late life or
49 during their terminal year. Therefore, the results suggest changes that changes in the GM
50 with age are not linked to senescence. Interestingly, we found an increase in the
51 abundance of a group of transposase genes with age, which may accumulate passively or
52 due to increased transposition induced as a result of stressors that arise with age. These
53 findings reveal taxonomic and functional GM changes with age in a wild vertebrate and
54 provide a blueprint for future wild functional GM studies linked to age and senescence.

55

56 **Keywords:** gut microbiome, age, senescence, metagenomics, transposase, *Acrocephalus*
57 *sechellensis*

58 Introduction

59

60 Senescence - a decline in physiological function in later life- occurs in most organisms
61 [1,2]. However, its onset and rate often differ greatly among individuals within populations
62 [1,3]. One factor that may contribute to individual differences in senescence is variation in
63 host-associated microbial communities. The intestinal tract of animals contains a diverse
64 collection of microbes and their genomes (the gut microbiome; GM), which play an
65 important role in host adaptation and fitness [4,5]. The GM influences the regulation of
66 essential processes, such as digestion, reproduction, and immune function [6,7]. However,
67 shifts in GM composition can be detrimental to the host; certain microbes may be
68 pathogenic, while overall dysbiosis may impair host function [8,9].

69

70 Studies in humans and laboratory animals have shown that GM composition generally
71 changes rapidly in early life [10,11] before stabilising during adulthood [12]. This is often
72 followed by greater GM instability in advanced age including a loss of diversity and
73 changes to composition [13–15]. These late-life compositional shifts are generally
74 characterised by a loss of commensal or probiotic bacteria and an increase in pathogenic
75 microbes [16]. GM functional changes with age have also been identified. For example,
76 healthy ageing has been associated with microbes that enable increased biodegradation
77 and metabolism of xenobiotics [16,17], whereas unhealthy ageing has been linked to
78 increased production of detrimental microbial metabolites [16].

79

80 Studies have demonstrated links between the GM and senescence in humans and
81 laboratory animals, however, their GM composition varies markedly from their counterparts
82 living in natural environments because of the artificial environments they are exposed to
83 [18,19]. It remains unclear if these effects can be generalised to wild animals [18–20].

84

85 Recent studies on wild organisms have not reached a consensus on what characterises
86 the ageing microbiome. Some have documented altered GM composition [21–23],
87 increased GM diversity [22,24], and reduced GM stability [25] with increasing age. Other
88 studies have indicated that GM characteristics remain relatively stable throughout
89 adulthood [25–27]. However, these studies have been based on 16S rRNA gene
90 metabarcoding, which is limited in resolution [28–30]. Shotgun metagenomic sequencing
91 enables higher taxonomic resolution (species or strain level), as well as informing on the
92 functional potential of microbial communities based on gene content [31–33]. In humans
93 and captive primates, metagenomics has revealed an increase in pathogenic microbial
94 genes, and a decrease in beneficial genes, with age [17,34,35]. To our knowledge, no
95 previous studies have investigated GM functional changes with age and senescence using
96 shotgun metagenomics in a wild population.

97

98 Also, most GM studies on wild animals have relied on a cross-sectional sampling of
99 differently aged individuals [36–38] and, therefore, may be confounded by the selective

100 appearance/disappearance of individuals with particular GM characteristics. A lack of
101 longitudinal samples also makes it difficult to infer changes in GM stability with age [39].
102 Understanding what drives this GM variation is important, as it may lead to a deeper
103 comprehension of the evolution of senescence and life-history trade-offs [3], and enhance
104 our ability to prolong healthy lifespans. As senescence occurs at different rates across
105 individuals, a longitudinal approach is crucial for accurately evaluating age-associated
106 effects [40]. Given this rate variation, and because declines are expected to be greatest at
107 the end of life, GM changes may be more closely associated with proximity to death than
108 chronological age. Including such information in analyses requires accurate estimates of
109 the point of death that are not confounded by dispersal.

110
111 The long-term study of the Seychelles warbler population on Cousin Island provides a
112 powerful natural system in which to study GM variation and host senescence [3]. Its
113 isolated nature allows for the longitudinal sampling of uniquely marked, known-age
114 individuals across their entire lifespan and the collection of accurate survival and
115 reproductive success data [41,42]. Previous studies using 16S metabarcoding have
116 demonstrated that Seychelles warbler GM composition is linked to subsequent survival
117 [43] but identified no overall patterns of GM senescence [26].

118
119 Here, we use shotgun metagenomics to assess fine-scale changes in the GM with age and
120 senescence in the Seychelles warbler. First, we determine how GM taxonomic diversity
121 and composition change with host age, particularly in a bird's terminal year when GM
122 dysregulation is expected to be at its greatest. Then we test the hypothesis that GM
123 functional characteristics (assessed via microbiome gene content) will change with age,
124 senescence, and in the terminal year.

125

126 **Materials and Methods**

127

128 **Study system and sample collection**

129 Seychelles warblers are insectivorous passerines endemic to the Seychelles archipelago.
130 The population on Cousin Island (29 ha; 04° 20' S, 55° 40' E) has been extensively
131 monitored since 1985 in the winter (January – March) and summer (June – October)
132 breeding seasons [3,44,45]. Each season nearly all new birds (offspring) are caught, in the
133 nest or as dependent fledglings in the natal territory [45]. As many adult birds as possible
134 are re-caught each season using mist nets. Bird age is determined using either
135 lay/fledgling date [45] for the majority of individuals, if birds are first caught without a
136 fledging date being recorded, eye colour is used to estimate age instead (see [45]).

137

138 The population on Cousin Island consists of ca. 320 individuals grouped into ca. 115
139 territories, defended year-round by a dominant breeding pair [46,47]. Territory quality is
140 calculated each season using arthropod counts, vegetation density, and territory size
141 information [45,48].

142

143 Nearly every bird in the population (> 96% since 1997 [49]) has been caught and marked
144 with a unique combination of a British Trust for Ornithology (BTO) metal ring and three
145 plastic colour rings, which enables them to be monitored throughout their lives [3,50].
146 Individuals almost never disperse between islands and the annual resighting probability is
147 around 98% ± 1% [41,42,51]. If an individual is not seen for two consecutive seasons it is
148 assumed to have died (an error rate of 0.04%) [41,42]. Death dates for individuals were set
149 as the final day of the season in which the bird was last seen. Benign climatic conditions
150 and a lack of predators result in relatively long-lived individuals (median lifespan 5.5 years,
151 max lifespan 19 years) [46,52]. Extensive previous research shows that reproductive and
152 actuarial senescence occurs in this population (Hammers et al., 2015, 2019, 2021).

153

154 Faecal samples were collected from caught birds and stored as described previously (see
155 [26] and supplementary material). Contamination (hand) controls were collected from
156 fieldworkers each season. The time-of-day that samples were collected and the number of
157 days for which samples were stored at 4°C, were recorded. A ca 25 µl blood sample was
158 also taken via brachial venepuncture and stored in 1 mL of absolute ethanol at 4°C.

159

160 **DNA extraction and sequencing**

161 Blood samples were processed with a salt extraction method [42] or Qiagen DNeasy
162 Blood and Tissue Kit and the resulting DNA was used for molecular sexing [52,54].
163 DNA from faecal samples was extracted using the Qiagen DNeasy PowerSoil Kit with a
164 modified protocol (see [55]). Individuals for which multiple longitudinal samples were
165 available were prioritised for metagenomic sequencing to capture within-individual

166 changes. In total, 155 faecal samples from 92 individuals across 7 years were sequenced,
167 as well as three positive controls (two extractions from a ZymoBIOMICS Microbial
168 Community Standard (D6300), and one extraction from a ZymoBIOMICS Fecal Reference
169 with TruMatrix™ Technology (D6323)), and six hand controls. Library preparation was
170 performed in two lanes per run using the LITE protocol [56] and sequencing undertaken in
171 two runs of 2 x 150 bp NovaSeq X platform. The D6300 extraction control was sequenced
172 on both runs to compare extraction and batch effects.

173

174 **Bioinformatics**

175 Shotgun metagenomic sequence analysis was carried out using the MATAFILER pipeline
176 (see [5] and supplementary materials). Briefly, MATAFILER removes host reads,
177 assembles reads, predicts and annotates genes, builds metagenome-assembled genomes
178 (MAGs) and metagenomic species (MGSs), and taxonomically assigned MGSs. Due to the
179 high individuality of the Seychelles warbler GM and the high sequencing coverage
180 required to assign MGS, Metaphlan4 was also used to taxonomically classify reads (see
181 supplementary materials for details).

182

183 **Gut microbiome analyses**

184 A total of 162 samples were successfully processed bioinformatically (153 faecal samples,
185 4 controls). Positive controls were successfully recovered, and hand controls did not
186 contribute to substantial contamination in samples (Figure S1).

187

188 The 153 faecal samples (Figure S2) included 71 from 40 females and 82 from 51 males. In
189 total, 41 individuals had one sample, 41 had two, eight individuals had three, and one
190 individual had four samples. Age at sampling ranged from 0.6-17.0 years (mean 5.7 ± 0.3
191 SE). Of these, 48 were from 22 individuals in their terminal year (the year in which they
192 died); with ages in terminal year ranging from 1.4–17.0 years. From all these samples, 1025
193 unique metaphlan4 species-genome-bins assignments were used for the subsequent
194 taxonomic analysis (mean 29.3 ± 2.0 SE per sample).

195

196 All statistical analysis was performed using R version 4.33 [57,58]. Variance Inflation
197 Factor (VIF) scores (*car* version 3.1.2) were used to test for collinearity between variables
198 in all models; all had a score <3 indicating no issues with collinearity [59].

199

200 **Taxonomic GM changes with age**

201 Taxonomic GM alpha diversity

202

203 A rarefaction curve of Metaphlan4 species was constructed with *iNEXT* version 3.0.1 to
204 determine the read depth required to recover 95% of theoretically present species (Figure

205 S3) [60]. Taxonomic classifications were rarefied to a depth of 5,500 reads before alpha
206 diversity analysis; two samples were removed due to insufficient read depth. Species
207 richness and Shannon diversity metrics were calculated per sample using R packages
208 *phyloseq* version 1.46.0 and *microbiome* 1.24.0 [61,62]. Wilcoxon rank sum tests were
209 used to examine whether different sequencing plates affected species diversity (Shannon
210 index, $p = 0.353$) and species richness (Observed index, $p = 0.124$), both were not
211 significantly different.

212

213 A linear mixed effect model with a Gaussian distribution (*lmer*), and a generalised linear
214 mixed effect model with a negative binomial distribution (*glmer.nb*), were used to model
215 changes in species diversity (Shannon index) and richness (observed taxa), respectively,
216 using *lme4* version 1.1-35.5 [63]. Fixed effect variables included in models were: host age
217 (years); terminal year (yes/no); sex (male/female); breeding season (winter/summer);
218 sample year (as a factor: 2017-2023); territory quality; storage at 4°C (days); time of day
219 collected (minutes since sunrise at 6:00 am). Bird ID was included as a random effect. A
220 quadratic age term, and an interaction between terminal year and host age, were tested to
221 assess whether GM changes became more extreme in the terminal year but were dropped
222 if not significant to allow interpretation of the main effects. Age was measured in years, but
223 all samples taken when birds were >12 years of age were designated as 12 years because
224 these samples were rare ($n = 9$, max age = 17 years). Model diagnostics were run using
225 *DHARMA* version 0.4.6, with no significant issues in each chosen model [64]. Herein, all
226 models were tested with the same variables unless stated otherwise.

227

228 A within-subject centering approach was used to separate between-individual (cross-
229 sectional) GM differences with age (which could be driven by the selective
230 appearance/disappearance of individuals with particular GM characteristics), from within-
231 individual (longitudinal) change (which could indicate senescence) [65]. This involves
232 calculating the mean age of each individual across all its sampling events (mean age) and
233 the within-individual deviation from that mean age at each separate sampling event (delta
234 age). These terms replace host age in the model. The fixed effect of terminal year was also
235 replaced by a "terminal year bird" term (yes/no) which indicates whether individuals have
236 at least one sample collected in the terminal year or not. An interaction between the
237 terminal year bird and delta age, as well as quadratic delta age, were tested to assess
238 whether within-individual GM changes were more extreme in birds with a sample taken in
239 the terminal year of life and/or in older individuals, respectively (which would be indicative
240 of senescence). These were dropped if not significant to allow interpretation of the main
241 effects.

242

243 Taxonomic GM composition

244

245 A permutational multivariate analysis of variances (PERMANOVA) was carried out on a
246 Euclidean distance matrix calculated using centered log ratio (CLR)-transformed reads,

247 using the `adonis2()` function in *vegan* version 2.6.6 [66]. A blocking effect of Bird ID was
248 used to account for repeated measures. The same predictors were included as for the
249 main model in the Alpha diversity analysis above. Differences in composition were
250 visualised with a principal component analysis (PCA) in *phyloseq* version 1.46.0 [62].

251

252 Taxonomic GM differential abundance analysis (DAA)

253

254 Two different DAA methods were used to identify differentially abundant GM species with
255 host age (as recommended by [67,68]; *ANCOMBC2* version 2.4.0 and *GLLVM* version
256 1.4.3 [69,70]). A total of 22 common species, defined as species found in 20% of the
257 population at more than 0.01% abundance, were retained. Species that were significantly
258 differentially abundant in the same direction using both DAA methods were considered
259 robustly significant. Variables included in each model were the same as in models above.

260

261 **Functional GM changes with age**

262 Functional GM alpha diversity

263

264 Initially, 4727 different eggNOG orthologues (mean = 3616.6 ± 64.4 SE per sample) were
265 identified in our gene catalogues. A rarefaction curve of eggNOG orthologues was
266 constructed using *iNEXT* to determine sample completeness [60]. Samples were then
267 rarefied to 100,000 reads based on >95% completeness. One sample was removed due
268 to insufficient reads. Following rarefaction, 4685 eggNOG orthologues were retained
269 (mean = 3054.3 ± 47.1 SE per sample). Due to the (negative) skewness of the observed
270 richness and Shannon diversity of eggNOG annotations, a scaled exponential
271 transformation and an exponential transformation were used for analyses, respectively, to
272 improve residual fit. Both these alpha diversity indices were then analysed with linear
273 mixed models containing the same predictors as for taxonomic alpha diversity above.

274

275 Functional GM composition

276

277 To test for changes in functional microbiome beta diversity, a PERMANOVA of Euclidean
278 distances calculated from CLR-transformed read abundances per orthologue was used,
279 using the same model structure as for taxonomic compositional analysis (described
280 above). Differences in composition were visualized with a PCA plot as above.

281

282 Functional GM differential abundance analysis (DAA)

283

284 Differential abundance analysis was performed on eggNOG annotations using their
285 assigned categories from the database of clusters of orthologous genes (COG)
286 (Supplementary Table S5) [71] using *ANCOMBC2* and *GLLVM* as described above
287 [69,70]. Post-hoc DAA were performed on individual eggNOG members found within

288 differentially abundant COG categories to establish the drivers of any significant
289 differences (see Supplementary material for details).

290 **Results**

291

292 **Taxonomic GM changes with age**

293 Taxonomic GM alpha diversity

294

295 GM species richness declines with host age, and individuals in their terminal year had
296 significantly lower species richness than those in a non-terminal year (Table S1 & Figure
297 S4). However, Shannon diversity was not significantly associated with host age, and did
298 not differ between samples taken in a terminal or non-terminal year (Table S2). A quadratic
299 age term, and an interaction between host age and terminal year were not significantly
300 associated with species richness or Shannon diversity ($p > 0.05$) and were dropped from
301 the final model.

302

303 The within-individual centering approach revealed that the decline in GM species richness
304 with host age occurred longitudinally within individuals (Table 1, Figure 1) with no evidence
305 of between-individual selective disappearance effects (Table 1). Shannon diversity did not
306 change significantly with mean or delta age (Table S3). There was no evidence of a
307 quadratic relationship between within-individual delta age and species richness or
308 Shannon diversity, hence the quadratic age term was dropped from the final model. This
309 suggests that within-individual changes were not more extreme in older individuals and
310 that declines in species richness happen equally in all mature individuals. We also tested
311 for an interaction between within-individual age and whether an individual's final sample
312 was in their terminal year, but this was not significant ($p > 0.05$) and was dropped. This
313 result indicates that within-individual changes in species richness with age had a similar
314 slope whether the bird was sampled in its terminal year or not.

315

316 Taxonomic GM composition

317 A PERMANOVA analysis found that cross-sectional host age was a marginally significant
318 predictor of GM taxonomic composition (Table 2), but terminal year was not (Table 2).
319 Sample year, season, and catch time were significant and explain the largest proportion of
320 GM compositional variance (Table 2) followed by days sample stored at at 4°C and sex. An
321 interaction between age and terminal year was not significant ($p > 0.05$). A PCA showed
322 limited sample clustering according to age, which is consistent with the small amount of
323 variance explained in the PERMANOVA (Figure S5).

324

325 Taxonomic GM differential abundance analysis (DAA)

326 Five of the 22 common GM species found in the Seychelles warbler population (i.e. in
327 >20% individuals) differed significantly in relative abundance with age in the GLLVM
328 analysis (*Escherichia coli*, *Lactococcus lactis*, *Brucella pseudogrignonensis*, *Lactococcus*
329 *garvieae*, *Microbacterium enclense*), but none were differentially abundant with age in the
330 ANCOMBC2 analysis (Figure S6A & S6B). Similarly, six species were differentially

331 abundant in the terminal year in the GLLVM analysis (*Lactococcus garvieae*, *Pantoea*
332 *anthophila*, *Escherichia coli*, *Rothia* sp AR01, *Microbacterium enclense*, *Brucella*
333 *pseudogrignonensis*), but none were differentially abundant with terminal year in the
334 ANCOMBC2 analysis (Figure S6C & S6D). Thus, there is no clear consensus of significant
335 variation in the abundance of specific GM species with age or in the terminal year.
336

337 **Functional GM changes with age**

338

339 Functional GM alpha diversity

340

341 Alpha diversity of eggNOG gene orthologues declined significantly with host age for both
342 observed richness and Shannon diversity metrics (Table S4, Figure S7). Alpha diversity of
343 eggNOG orthologues did not differ between terminal year and non-terminal year samples
344 (Table S4). Additionally, the interaction between host age (or quadratic age) and terminal
345 year was not significant ($p > 0.05$).

346

347 The decrease in functional alpha diversity with host age is best explained by within-
348 individual longitudinal changes with age for both tested indices (Table 3, Figure 2). Cross-
349 sectional, between-individual age was a marginally significant predictor of Shannon
350 diversity but not observed richness. Alpha diversity did not differ between individuals that
351 had at least one sample taken in their terminal year and those that did not. The interaction
352 of terminal year bird and within-individual age as well as quadratic within-individual age
353 were also not significant ($p > 0.05$) predictors of either index. Sample year was a
354 significant variable of both eggNOG observed richness and Shannon diversity.
355

356

356 Functional GM beta diversity

357 A PERMANOVA analysis identified factors that were significantly related to GM functional
358 composition (Table 4). Host age, but not terminal year, was a marginally significant
359 predictor of functional composition (Table 4). An interaction between age and terminal
360 year was not significant ($p > 0.05$). The largest effect sizes were found in relation to
361 season, sample year, sex, and days stored at 4°C (Table 4). Time of day was not significant
362 related to GM functional composition (in contrast to GM taxonomic composition). A PCA
363 plot showed limited clustering of GM samples according to age, consistent with the small
364 amount of variance explained by this variable (Figure S8).
365

366

366 Functional GM differential abundance analysis (DAA)

367 Only one cluster of orthologous genes (COG) category was differentially abundant in
368 relation to age. The COG category "X", which represents mobilome COGs such as
369 prophages and transposons, significantly increased in abundance with age in both the
370 ANCOMBC2 and the GLLVM analyses (Figure 3). Several COG categories were
371 significantly differentially abundant with environmental variables including Cat A (RNA

372 processing and modification) with season and Cat C (Energy production and conversion)
373 with sample year (Figure S10, Figure S11).

374

375 Within category X (mobilome), only COG2801 (transposase genes) was found to
376 significantly increase in abundance with age in both GLLVM and ANCOMBC2 analyses
377 (Figure S9). A within-subject centering approach within a linear mixed model showed an
378 increase in COG2801 was associated with both within-individual (longitudinal) age and
379 between-individual (cross-sectional) age (Table S7, Figure 4). However, the interaction
380 between within-individual age and terminal year was not significant ($p > 0.05$).

381

382 COG2801 located within MGSs (509 COG2801 copies from 160 MGS) were most closely
383 related to the group insertion sequences (IS) 3 family of transposases (30%), other IS
384 family transposases (12%), partial or putative transposases (33%) or other/unknown
385 function (25%; Table S8). An increased abundance of COG2801 in the GM may be due to
386 either an increase in the abundance of COG2801-carrying microbes or increased
387 replication of the transposase gene itself. However, contrary to the first hypothesis, we
388 found no relationship between the total abundance of COG2801-carrying MGSs ($n = 160$)
389 and host age (Table S9). To further test this, COG2801-MGSs were matched with
390 metaphlan4 annotations at the genus level; the abundance of COG2801-metaphlan4
391 genera was not significantly associated with host age (Table S10). Hence, the increase in
392 COG2801 abundance with host age could not be attributed to an increased abundance of
393 COG2801-carrying bacteria. Additionally, within COG2801, ten gene catalogues were
394 commonly shared across 50% of samples. Each of these ten COG2801 gene catalogues
395 was not significantly ($p > 0.05$) differentially abundant with age individually when tested
396 using both ANCOMBC2 or GLLVM analysis (Figure S12). Thus, the increase in abundance
397 of COG2801 with age was not being driven by the abundance of a single prevalent, gene
398 catalogue but rather the cumulative abundance of many.

399 Discussion

400

401 We used a longitudinal metagenomic dataset from individuals in a Seychelles warbler
402 population to investigate how GM taxonomic and functional characteristics varied with
403 host age. We identified a linear decrease in species richness, and small shifts in GM
404 taxonomic composition, with host age. Additionally, species richness was lower in samples
405 taken during an individual's terminal year, but taxonomic composition did not differ
406 between terminal and non-terminal samples. We also identified a linear decrease in the
407 GM's functional richness and diversity, and differences in functional GM composition, with
408 host age. Finally, COG categories representing the mobilome increased in prevalence with
409 bird age, driven by an increase in the abundance of COG2801, a group of transposases.

410

411 The small reduction in GM richness, but not Shannon diversity, with age suggests a loss of
412 rare taxa that is not linked with a major restructuring of the evenness of the GM. This also
413 concurs with the small changes in GM composition with age we identified; i.e showing a
414 limited number of differentially abundant taxa with increasing host age. This result is
415 consistent with a previous 16S metabarcoding analysis of senescence of the Seychelles
416 warbler GM despite the increased taxonomic resolution afforded by a metagenomics
417 approach [26] Overall, the results support the conclusion that, taxonomically, most of the
418 GM stays the same with increasing age, apart from the loss of a few rare taxa.

419

420 Taxonomic changes in GM species diversity and composition with age have been
421 repeatedly demonstrated in humans and captive animals [16]. However, in these species,
422 late-life changes in the GM may be due to external factors such as antibiotic use, lifestyle,
423 and dietary changes [18,20]. An increasing number of wild animal studies are finding little
424 evidence of a late-life shift in GM taxonomic diversity without such external factors (see
425 [26,72]). Our study supports this conclusion despite the longitudinal sampling and
426 increased resolution yielded by shotgun metagenomics, which can potentially reveal more
427 nuanced changes at lower taxonomic levels.

428

429 Few studies have directly investigated functional changes in the GM with age in wild
430 animals [73]. Some studies have been undertaken using functional inferences from
431 metabarcoding sequence homology. However, this can be misleading due to being limited
432 to variation within the same genus thus providing potentially inaccurate functional profiles.
433 [74,75]. In our study using a higher resolution metagenomic approach, we found evidence
434 of small, linear, changes in GM functional diversity and composition with age in the
435 Seychelles warbler. Functional observed richness and Shannon diversity declined with
436 age, which suggests not only that rare functions are lost, but that the evenness of these
437 GM functions also changes linearly with adult age. Age-related decreases in functional
438 richness and shifts in functional composition have previously been identified in elderly
439 humans [76,77]. Such changes have been linked to the onset of specific disease states,

440 such as inflammation and pathogenesis and changes to diet degradation and digestion, in
441 humans and laboratory mice [78]. However, other studies have either found no change in
442 functional alpha diversity, or even an increase in microbial functional richness and diversity
443 with age [35,79]. Whether the loss of functional diversity, and minor changes in functional
444 composition, with host age in Seychelles warbler is linked to declines in health and
445 condition remains unclear and requires further study.

446
447 Despite the small changes in functional diversity and composition with age in the
448 Seychelles warbler, we only identified one specific functional category whose abundance
449 was significantly associated with host age. An increase in the abundance of COG2801
450 transposases occurred with age. However, this was not due to an increase in COG2801-
451 carrying microbes. COG2801 are a group of transposases that are primarily found in
452 bacteria (89.5%) and have been shown to be the most widely transferred genes among
453 prokaryotes [80]. Most COG2801 genes found within MGSs were group insertion
454 sequences 3 (IS3), which use a copy-out-paste-in mechanism to replicate [81]. This could
455 lead to an increased number of transposon copies in the same individual bacterial genome
456 over time, or to horizontally transfer to other bacterial genomes. [82,83]. Thus, the
457 increased abundance of COG2801 with age in Seychelles warbler GM's may be the result
458 of self-replication, independent of microbial host cell DNA replication. An increase in
459 transposition has been observed when bacteria are stressed and COG2801 is one of the
460 most horizontally transferable eggNOG genes [84,85]. Therefore, as vertebrate hosts get
461 older, the GM may be exposed to a greater number or intensity of stressors, such as mucus
462 barrier thinning or inflammation, which may induce activation of COG2801 [86]. However,
463 there was not an accelerated increase (i.e. a quadratic relationship) of COG2801
464 abundance with host age, which would be expected if the cumulative effects of host
465 senescence were driving these changes. Therefore, stressors to the host that occur
466 linearly in adulthood, such as cell death in the gastrointestinal autonomic nervous system
467 [87,88], may better explain the increased abundance of COG2801 with host age

468
469 We also focused on assessing terminal year effects in the Seychelles warbler GM. Only
470 species richness was found to be significantly lower in the final year of a bird's life.
471 Moreover, the effect of terminal year was uniform across age, i.e. it was not more extreme
472 in older individuals. Previous research has identified age-dependent terminal-declines in
473 fitness components (reproductive success and survival probability) in the Seychelles
474 warbler [89]. However, the lack of age-dependent terminal changes in GM characteristics
475 identified in our study suggests that the GM does not undergo senescence in association
476 with these other traits. As such, the declines in microbial species richness in terminal year
477 samples (and linearly with age) may rather reflect the stabilisation of the GM with age
478 rather than a senescence effect. These results concur with the previous 16S
479 metabarcoding analysis of the Seychelles warbler GM which found little evidence of GM
480 senescence [26].

481

482 Across analyses, environmental factors explained most of the variance in the Seychelles
483 warbler GM. This concurs with previous research on this species [26,43,55] as well as
484 studies of other taxa [21,90,91]. Temporal variation -specifically year and season-
485 explained the most variance in both taxonomic and functional GM composition. This may
486 be explained by many factors including climate variability, differences in insect prey
487 availability, or host population density [92–94]. Most Seychelles warbler individuals breed
488 in the summer rather than the winter season, and GM shifts may therefore reflect
489 reproductive activity and related hormonal changes [24]. Time of day was also associated
490 with GM composition. Differences in insect activity might drive this pattern due to light
491 availability and/or temperature [95,96]. However, such patterns could also be due to host
492 intrinsic circadian rhythms [97]. These factors lead to a substantial amount of noise in GM
493 studies that can confound studies on ageing, reproduction, and disease outcomes in wild
494 populations. Therefore, accounting for these factors is important when investigating the
495 GM in natural systems.

496
497 Our findings highlight the need for more studies investigating the functional characteristics
498 of wild microbiomes as taxonomic relationships might not capture functional GM changes
499 that occur (e.g. the increased prevalence of COG2801). However, researchers should not
500 totally discount the utility of 16S metabarcoding for investigating general GM questions, as
501 it may, in many cases, provide sufficient taxonomic resolution to answer specific questions
502 [28]. Indeed, we identified similar taxonomic patterns using shotgun metagenomics to
503 those revealed by a previous metabarcoding study on the Seychelles warbler [26]. The
504 cost-effectiveness of 16S rRNA allows greater sample sizes, and thus power, to resolve
505 certain questions. A combination approach that harmonises both 16S metabarcoding and
506 shotgun metagenomics has been proposed to maximise sample size, although such
507 analyses are limited to genus-level comparisons [98]. On the other hand, shotgun
508 metagenomics not only allows higher taxonomic resolution and functional analysis of the
509 GM, but also an assessment of the interaction between taxa and their functions. As
510 described with transposable elements, our functional analysis uncovered changes in GM
511 function that were not detectable using 16S metabarcoding analysis.

512
513 In conclusion, while we found that the Seychelles warbler GM changes in terms of
514 diversity, composition and even function with age, this happens gradually over the adult
515 lifespan and there is little evidence of late-life GM senescence. Whilst species richness is
516 lower in the terminal year, this occurs at all ages and is not more extreme in the oldest
517 individuals. Interestingly, we found that the abundance of a group of transposase gene
518 increases considerably with age in the GM, probably because of more frequent
519 transposition within the GM community over time. Future work is required to determine
520 exactly why these transposable element changes occur and what impact they may have.
521 Additionally, work should investigate the generality of these conclusions by assessing
522 whether functional changes occur in the GM of other wild vertebrates.

523

524 **References**

- 525 1. Nussey DH, Froy H, Lemaître JF *et al.* Senescence in natural populations of animals:
526 Widespread evidence and its implications for bio-gerontology. *Ageing Res Rev*
527 2013;**12**:214–25.
- 528 2. Jones OR, Scheuerlein A, Salguero-Gómez R *et al.* Diversity of ageing across the tree of
529 life. *Nature* 2014;**505**:169–73.
- 530 3. Hammers M, Kingma SA, Bebbington K *et al.* Senescence in the wild: Insights from a
531 long-term study on Seychelles warblers. *Exp Gerontol* 2015;**71**:69–79.
- 532 4. Petersen C, Hamerich IK, Adair KL *et al.* Host and microbiome jointly contribute to
533 environmental adaptation. *ISME Journal* 2023;**17**:1953–65.
- 534 5. Hildebrand F, Gossmann TI, Frioux C *et al.* Dispersal strategies shape persistence and
535 evolution of human gut bacteria. *Cell Host Microbe* 2021;**29**:1167–1176.e9.
- 536 6. Cholewińska P, Czyż K, Nowakowski P *et al.* The microbiome of the digestive system of
537 ruminants – a review. *Anim Health Res Rev* 2020;**21**:3–14.
- 538 7. Caviedes-Vidal E, McWhorter TJ, Lavin SR *et al.* The digestive adaptation of flying
539 vertebrates: High intestinal paracellular absorption compensates for smaller guts.
540 *Proceedings of the National Academy of Sciences* 2007;**104**, DOI:
541 10.1073/pnas.0703159104.
- 542 8. Thevaranjan N, Puchta A, Schulz C *et al.* Age-Associated Microbial Dysbiosis Promotes
543 Intestinal Permeability, Systemic Inflammation, and Macrophage Dysfunction. *Cell Host*
544 *Microbe* 2017;**21**:455–466.e4.
- 545 9. Davenport ER, Sanders JG, Song SJ *et al.* The human microbiome in evolution. *BMC*
546 *Biol* 2017;**15**, DOI: 10.1186/s12915-017-0454-7.
- 547 10. Blyton MDJ, Soo RM, Hugenholtz P *et al.* Maternal inheritance of the koala gut
548 microbiome and its compositional and functional maturation during juvenile development.
549 *Environ Microbiol* 2022;**24**:475–93.
- 550 11. Guard BC, Mila H, Steiner JM *et al.* Characterization of the fecal microbiome during
551 neonatal and early pediatric development in puppies. *PLoS One* 2017;**12**, DOI:
552 10.1371/journal.pone.0175718.
- 553 12. Dong B, Gazzano A, Garrigues Q. *Gut Microbiota Development in the Growing Dog: A*
554 *Dynamic Process Influenced by Maternal, Environmental and Host Factors.*, 2022.
- 555 13. Biagi E, Franceschi C, Rampelli S *et al.* Gut Microbiota and Extreme Longevity. *Current*
556 *Biology* 2016;**26**, DOI: 10.1016/j.cub.2016.04.016.
- 557 14. Maynard C, Weinkove D. The Gut Microbiota and Ageing. 2018, 351–71.
- 558 15. Dillin A, Smith P, Willemsen D *et al.* Regulation of life span by the gut microbiota in the
559 short-lived African turquoise killifish. 2017, DOI: 10.7554/eLife.27014.001.
- 560 16. Ghosh TS, Shanahan F, O'Toole PW. The gut microbiome as a modulator of healthy
561 ageing. *Nat Rev Gastroenterol Hepatol* 2022;**19**:565–84.
- 562 17. Rampelli S, Soverini M, D'Amico F *et al.* Shotgun Metagenomics of Gut Microbiota in
563 Humans with up to Extreme Longevity and the Increasing Role of Xenobiotic Degradation.
564 *mSystems* 2020;**5**, DOI: 10.1128/msystems.00124-20.
- 565 18. Gibson KM, Nguyen BN, Neumann LM *et al.* Gut microbiome differences between wild
566 and captive black rhinoceros – implications for rhino health. *Sci Rep* 2019;**9**, DOI:
567 10.1038/s41598-019-43875-3.
- 568 19. Reese AT, Chadaideh KS, Diggins CE *et al.* Effects of domestication on the gut
569 microbiota parallel those of human industrialization. *Elife* 2021;**10**, DOI:
570 10.7554/eLife.60197.

- 571 20. Oliveira BCM, Murray M, Tseng F *et al.* The fecal microbiota of wild and captive raptors.
572 *Anim Microbiome* 2020;**2**, DOI: 10.1186/s42523-020-00035-7.
- 573 21. Ren T, Boutin S, Humphries MM *et al.* Seasonal, spatial, and maternal effects on gut
574 microbiome in wild red squirrels. *Microbiome* 2017;**5**:163.
- 575 22. Fenn J, Taylor C, Goertz S *et al.* Discrete patterns of microbiome variability across
576 timescales in a wild rodent population. *BMC Microbiol* 2023;**23**, DOI: 10.1186/s12866-
577 023-02824-x.
- 578 23. Pannoni SB, Proffitt KM, Holben WE. Non-invasive monitoring of multiple wildlife health
579 factors by fecal microbiome analysis. *Ecol Evol* 2022;**12**, DOI: 10.1002/ece3.8564.
- 580 24. Hernandez J, Hucul C, Reasor E *et al.* Assessing age, breeding stage, and mating
581 activity as drivers of variation in the reproductive microbiome of female tree swallows. *Ecol*
582 *Evol* 2021;**11**:11398–413.
- 583 25. Sadoughi B, Schneider D, Daniel R *et al.* Aging gut microbiota of wild macaques are
584 equally diverse, less stable, but progressively personalized. *Microbiome* 2022;**10**, DOI:
585 10.1186/s40168-022-01283-2.
- 586 26. Worsley SF, Davies CS, Lee CZ *et al.* Longitudinal gut microbiome dynamics in relation
587 to age and senescence in a wild animal population. *Mol Ecol* 2024, DOI:
588 10.1111/mec.17477.
- 589 27. Baniel A, Amato KR, Beehner JC *et al.* Seasonal shifts in the gut microbiome indicate
590 plastic responses to diet in wild geladas. *Microbiome* 2021;**9**:26.
- 591 28. Durazzi F, Sala C, Castellani G *et al.* Comparison between 16S rRNA and shotgun
592 sequencing data for the taxonomic characterization of the gut microbiota. *Sci Rep* 2021;**11**,
593 DOI: 10.1038/s41598-021-82726-y.
- 594 29. Scholz MB, Lo C-C, Chain PS. Next generation sequencing and bioinformatic
595 bottlenecks: the current state of metagenomic data analysis. *Curr Opin Biotechnol*
596 2012;**23**:9–15.
- 597 30. Worsley SF, Mazel F, Videvall E *et al.* *Probing the Functional Significance of Wild*
598 *Animal Microbiomes Using Omics Data.*, 2024.
- 599 31. Hugenholtz P, Tyson GW. Metagenomics. *Nature* 2008;**455**:481–3.
- 600 32. Cerk K, Ugalde-Salas P, Nedjad CG *et al.* Community-scale models of microbiomes:
601 Articulating metabolic modelling and metagenome sequencing. *Microb Biotechnol*
602 2024;**17**, DOI: 10.1111/1751-7915.14396.
- 603 33. Frioux C, Singh D, Korcsmaros T *et al.* From bag-of-genes to bag-of-genomes:
604 metabolic modelling of communities in the era of metagenome-assembled genomes.
605 *Comput Struct Biotechnol J* 2020;**18**:1722–34.
- 606 34. Duan J, Yin B, Li W *et al.* Age-related changes in microbial composition and function in
607 cynomolgus macaques. *Aging* 2019;**11**:12080–96.
- 608 35. Rampelli S, Candela M, Turrone S *et al.* Functional metagenomic profiling of intestinal
609 microbiome in extreme ageing. *Aging* 2013;**5**:902–12.
- 610 36. Bennett G, Malone M, Sauter ML *et al.* Host age, social group, and habitat type
611 influence the gut microbiota of wild ring-tailed lemurs (*Lemur catta*). *Am J Primatol*
612 2016;**78**:883–92.
- 613 37. Janiak MC, Montague MJ, Villamil CI *et al.* Age and sex-associated variation in the
614 multi-site microbiome of an entire social group of free-ranging rhesus macaques.
615 *Microbiome* 2021;**9**, DOI: 10.1186/s40168-021-01009-w.
- 616 38. Pereira AC, Bandeira V, Fonseca C *et al.* Egyptian mongoose (*Herpestes ichneumon*)
617 gut microbiota: Taxonomical and functional differences across sex and age classes.
618 *Microorganisms* 2020;**8**, DOI: 10.3390/microorganisms8030392.

- 619 39. Chen L, Wang D, Garmaeva S *et al.* The long-term genetic stability and individual
620 specificity of the human gut microbiome. *Cell* 2021;**184**:2302-2315.e12.
- 621 40. Nussey DH, Coulson T, Festa-Bianchet M *et al.* Measuring Senescence in Wild Animal
622 Populations: Towards a Longitudinal Approach THE EVOLUTIONARY ECOLOGY OF
623 SENESCENCE Measuring senescence in wild animal populations: towards a longitudinal
624 approach. *Funct Ecol* 2008;**22**:393-406.
- 625 41. Raj Pant S, Hammers M, Komdeur J *et al.* Age-dependent changes in infidelity in
626 Seychelles warblers. *Mol Ecol* 2020;**29**:3731-46.
- 627 42. Richardson DS, Jury FL, Blaakmeer K *et al.* Parentage assignment and extra-group
628 paternity in a cooperative breeder: The Seychelles warbler (*Acrocephalus sechellensis*).
629 *Mol Ecol* 2001;**10**:2263-73.
- 630 43. Worsley SF, Davies CS, Mannarelli M-E *et al.* Gut microbiome composition, not alpha
631 diversity, is associated with survival in a natural vertebrate population. *Anim Microbiome*
632 2021;**3**:84.
- 633 44. Brown TJ, Dugdale HL, Hammers M *et al.* Seychelles warblers with silver spoons:
634 Juvenile body mass is a lifelong predictor of annual survival, but not annual reproduction or
635 senescence. *Ecol Evol* 2022;**12**:e9049.
- 636 45. Komdeur J. Importance of habitat saturation and territory quality for evolution of
637 cooperative breeding in the Seychelles warbler. *Nature* 1992;**358**, DOI:
638 10.1038/358493a0.
- 639 46. Hammers M, Kingma SA, Spurgin LG *et al.* Breeders that receive help age more slowly
640 in a cooperatively breeding bird. *Nat Commun* 2019;**10**:1301.
- 641 47. Komdeur J, Pels MD. Rescue of the Seychelles warbler on Cousin Island, Seychelles:
642 The role of habitat restoration. *Biol Conserv* 2005;**124**:15-26.
- 643 48. Brouwer L, Tinbergen JM, Both C *et al.* Experimental evidence for density-dependent
644 reproduction in a cooperatively breeding passerine. *Ecology* 2009;**90**, DOI: 10.1890/07-
645 1437.1.
- 646 49. Raj Pant S, Komdeur J, Burke TA *et al.* Socio-ecological conditions and female
647 infidelity in the Seychelles warbler. *Behavioral Ecology* 2019;**30**:1254-64.
- 648 50. Davies CS, Taylor MI, Hammers M *et al.* Contemporary evolution of the innate immune
649 receptor gene *TLR3* in an isolated vertebrate population. *Mol Ecol* 2021;**30**:2528-42.
- 650 51. Komdeur J, Piersma T, Kraaijeveld K *et al.* Why Seychelles Warblers fail to recolonize
651 nearby islands: unwilling or unable to fly there? *Ibis* 2004;**146**:298-302.
- 652 52. Sparks AM, Spurgin LG, van der Velde M *et al.* Telomere heritability and parental age at
653 conception effects in a wild avian population. *Mol Ecol* 2022;**31**:6324-38.
- 654 53. Hammers M, Kingma SA, van Boheemen LA *et al.* Helpers compensate for age-related
655 declines in parental care and offspring survival in a cooperatively breeding bird. *Evol Lett*
656 2021;**5**:143-53.
- 657 54. Griffiths R, Double MC, Orr K *et al.* A DNA test to sex most birds. *Mol Ecol*
658 1998;**7**:1071-5.
- 659 55. Davies CS, Worsley SF, Maher KH *et al.* Immunogenetic variation shapes the gut
660 microbiome in a natural vertebrate population. *Microbiome* 2022;**10**:41.
- 661 56. Perez-Sepulveda BM, Heavens D, Pulford C V. *et al.* An accessible, efficient and global
662 approach for the large-scale sequencing of bacterial genomes. *Genome Biol* 2021;**22**,
663 DOI: 10.1186/s13059-021-02536-3.
- 664 57. R Core Team. R: A Language and Environment for Statistical Computing. 2024.
- 665 58. Posit team. RStudio: Integrated Development Environment for R. 2024.

666 59. Fox John, Weisberg Sanford. *An R Companion to Applied Regression_*. Third.
667 Thousand Oaks, CA: Sage, 2019.

668 60. Chao A, Gotelli NJ, Hsieh TC *et al*. Rarefaction and extrapolation with Hill numbers: A
669 framework for sampling and estimation in species diversity studies. *Ecol Monogr*
670 2014;**84**:45–67.

671 61. Leo Lahti, Sudarshan Shetty. microbiome R package. 2019.

672 62. McMurdie PJ, Holmes S. Phyloseq: An R Package for Reproducible Interactive Analysis
673 and Graphics of Microbiome Census Data. *PLoS One* 2013;**8**, DOI:
674 10.1371/journal.pone.0061217.

675 63. Bates D, Mächler M, Bolker BM *et al*. Fitting linear mixed-effects models using lme4. *J*
676 *Stat Softw* 2015;**67**, DOI: 10.18637/jss.v067.i01.

677 64. Florian Hartig. DHARMA: Residual Diagnostics for Hierarchical (Multi-Level / Mixed)
678 Regression Models. 2022.

679 65. van de Pol M, Verhulst S. Age-Dependent Traits: A New Statistical Model to Separate
680 Within- and Between-Individual Effects. *Am Nat* 2006;**167**:766–73.

681 66. Oksanen Jari, Simpson Gavin L., Guillaume Blanchet F *et al*. vegan: Community
682 Ecology Package. 2024.

683 67. Nearing JT, Douglas GM, Hayes MG *et al*. Microbiome differential abundance methods
684 produce different results across 38 datasets. *Nat Commun* 2022;**13**, DOI:
685 10.1038/s41467-022-28034-z.

686 68. Cappellato M, Baruzzo G, Camillo B Di. Investigating differential abundance methods in
687 microbiome data: A benchmark study. *PLoS Comput Biol* 2022;**18**, DOI:
688 10.1371/journal.pcbi.1010467.

689 69. Lin H, Peddada S Das. Multigroup analysis of compositions of microbiomes with
690 covariate adjustments and repeated measures. *Nat Methods* 2024;**21**:83–91.

691 70. Niku J, Hui FKC, Taskinen S *et al*. gllvm: Fast analysis of multivariate abundance data
692 with generalized linear latent variable models in r. *Methods Ecol Evol* 2019;**10**:2173–82.

693 71. Tatusov RL, Galperin MY, Natale DA *et al*. *The COG Database: A Tool for Genome-*
694 *Scale Analysis of Protein Functions and Evolution.*, 2000.

695 72. Risely A, Schmid DW, Müller-Klein N *et al*. Gut microbiota individuality is contingent on
696 temporal scale and age in wild meerkats. *Proceedings of the Royal Society B: Biological*
697 *Sciences* 2022;**289**, DOI: 10.1098/rspb.2022.0609.

698 73. Levin D, Raab N, Pinto Y *et al*. Diversity and functional landscapes in the microbiota of
699 animals in the wild. *Science (1979)* 2021;**372**, DOI: 10.1126/SCIENCE.ABB5352.

700 74. Wilson ID, Nicholson JK. Gut microbiome interactions with drug metabolism, efficacy,
701 and toxicity. *Translational Research* 2017;**179**:204–22.

702 75. Chang Y, Li X, Ding L *et al*. Genetic and Functional Differences of Escherichia coli
703 Strains from Colorectal Cancer Mucosal Tissues. *Engineering* 2022;**16**:210–9.

704 76. Armour CR, Nayfach S, Pollard KS *et al*. *A Metagenomic Meta-Analysis Reveals*
705 *Functional Signatures of Health and Disease in the Human Gut Microbiome.*, 2019.

706 77. Mosca A, Leclerc M, Hugot JP. Gut microbiota diversity and human diseases: Should
707 we reintroduce key predators in our ecosystem? *Front Microbiol* 2016;**7**, DOI:
708 10.3389/fmicb.2016.00455.

709 78. Singh R, Zogg H, Wei L *et al*. Gut microbial dysbiosis in the pathogenesis of
710 gastrointestinal dysmotility and metabolic disorders. *J Neurogastroenterol Motil*
711 2021;**27**:19–34.

712 79. Ruiz-Ruiz S, Sanchez-Carrillo S, Ciordia S *et al.* Functional microbiome deficits
713 associated with ageing: Chronological age threshold. *Aging Cell* 2020;**19**, DOI:
714 10.1111/accel.13063.

715 80. Powell S, Forslund K, Szklarczyk D *et al.* EggNOG v4.0: Nested orthology inference
716 across 3686 organisms. *Nucleic Acids Res* 2014;**42**, DOI: 10.1093/nar/gkt1253.

717 81. Ohtsubo E, Minematsu H, Tsuchida K *et al.* INTERMEDIATE MOLECULES
718 GENERATED BY TRANSPOSASE IN THE PATHWAYS OF TRANSPOSITION OF
719 BACTERIAL INSERTION ELEMENT IS3., 2004.

720 82. Siguier P, Goubeyre E, Varani A *et al.* Everyman's Guide to Bacterial Insertion
721 Sequences. *Microbiol Spectr* 2015;**3**, DOI: 10.1128/microbiolspec.mdna3-0030-2014.

722 83. Wells JN, Feschotte C. A Field Guide to Eukaryotic Transposable Elements. *Annu Rev*
723 *Genet* 2020;**54**:539–61.

724 84. Lysnyansky I, Calcutt MJ, Ben-Barak I *et al.* Molecular characterization of newly
725 identified IS3, IS4 and IS30 insertion sequence-like elements in *Mycoplasma bovis* and
726 their possible roles in genome plasticity. *FEMS Microbiol Lett* 2009;**294**:172–82.

727 85. Nakamura Y. Prediction of Horizontally and Widely Transferred Genes in Prokaryotes.
728 *Evolutionary Bioinformatics* 2018;**14**, DOI: 10.1177/1176934318810785.

729 86. Elderman M, Sovran B, Hugenholtz F *et al.* The effect of age on the intestinal mucus
730 thickness, microbiota composition and immunity in relation to sex in mice. *PLoS One*
731 2017;**12**, DOI: 10.1371/journal.pone.0184274.

732 87. Phillips RJ, Pairitz JC, Powley TL. Age-related neuronal loss in the submucosal plexus
733 of the colon of Fischer 344 rats. *Neurobiol Aging* 2007;**28**:1124–37.

734 88. Phillips RJ, Powley TL. As the gut ages: Timetables for aging of innervation vary by
735 organ in the Fischer 344 rat. *Journal of Comparative Neurology* 2001;**434**:358–77.

736 89. Hammers M, Richardson DS, Burke T *et al.* Age-Dependent Terminal Declines in
737 Reproductive Output in a Wild Bird. *PLoS One* 2012;**7**:e40413.

738 90. Gacesa R, Kurilshikov A, Vich Vila A *et al.* Environmental factors shaping the gut
739 microbiome in a Dutch population. *Nature* 2022;**604**:732–9.

740 91. Wang Y, Xu B, Chen H *et al.* Environmental factors and gut microbiota: Toward better
741 conservation of deer species. *Front Microbiol* 2023;**14**, DOI:
742 10.3389/fmicb.2023.1136413.

743 92. Li H, Qu J, Li T *et al.* Pika population density is associated with the composition and
744 diversity of gut microbiota. *Front Microbiol* 2016;**7**, DOI: 10.3389/fmicb.2016.00758.

745 93. Sepulveda J, Moeller AH. The Effects of Temperature on Animal Gut Microbiomes.
746 *Front Microbiol* 2020;**11**, DOI: 10.3389/fmicb.2020.00384.

747 94. Foster EA, Franks DW, Morrell LJ *et al.* Social network correlates of food availability in
748 an endangered population of killer whales, *Orcinus orca*. *Anim Behav* 2012;**83**:731–6.

749 95. Welti EAR, Zajicek P, Frenzel M *et al.* Temperature drives variation in flying insect
750 biomass across a German malaise trap network. *Insect Conserv Divers* 2022;**15**:168–80.

751 96. Totland Ø, Totland E. Influence of Climate, Time of Day and Season, and Flower
752 Density on Insect Flower Visitation in Alpine Norway. *Arctic and Alpine Research*
753 1994;**26**:66–71.

754 97. Schmid DW, Capilla-Lasheras P, Dominoni DM *et al.* Circadian rhythms of hosts and
755 their gut microbiomes: Implications for animal physiology and ecology. *Funct Ecol*
756 2023;**37**:476–87.

757 98. Usyk M, Peters BA, Karthikeyan S *et al.* Comprehensive evaluation of shotgun
758 metagenomics, amplicon sequencing, and harmonization of these platforms for

759 epidemiological studies. *Cell Reports Methods* 2023;**3**, DOI:
760 10.1016/j.crmeth.2022.100391.
761
762

763 **Tables and figure legends**

764

765 Table 1. A generalised linear mixed effect model with a negative binomial distribution
 766 (glmer.nb) investigating gut microbiome species richness in relation to within- (delta) and
 767 between- (mean) individual variation in age amongst Seychelles warblers (n = 151
 768 samples, 91 individuals). Conditional R² = 47.1%. Reference categories for categorical
 769 variables are shown in brackets.

Predictor	Estimate	SE	z	P
(Intercept)	2.69	0.32	8.41	< 0.001
Delta Age	-0.13	0.06	-2.10	0.036
Mean Age	-0.03	0.02	-1.50	0.134
Terminal Year Bird (yes)	-0.19	0.14	-1.37	0.172
Season (winter)	0.00	0.16	-0.01	0.995
Sex (female)	-0.02	0.14	-0.11	0.916
Days at 4°C	-0.18	0.14	-1.31	0.190
Time of day	0.23	0.12	1.84	0.066
Territory quality	-0.07	0.13	-0.56	0.577
Sample Year (2017)				
2018	0.47	0.29	1.64	0.101
2019	0.45	0.33	1.38	0.169
2020	0.80	0.35	2.25	0.025
2021	0.76	0.34	2.21	0.027
2022	0.74	0.35	2.12	0.034
2023	0.89	0.40	2.20	0.028
Random				
Individual ID	151 observations	91 individuals	Variance	0.2075

770 Note: Significant (p < 0.05) predictors are shown in bold.

771

772 Table 2. A PERMANOVA analysis of gut microbiome taxonomic composition in relation to
 773 age and terminal year in the Seychelles warbler. The PERMANOVA was performed using a
 774 Euclidean distance matrix of CLR-transformed taxon abundances. N = 153 samples from
 775 91 individuals. Bird ID was included as a blocking factor.

Predictor	df	R ²	F	P
Age	1	0.009	1.368	0.043
Terminal Year	1	0.007	1.051	0.569
Season	1	0.013	2.021	0.001
Sample Year	6	0.056	1.479	< 0.001
Sex	1	0.007	1.096	0.064
Days at 4°C	1	0.008	1.193	0.034
Time of day	1	0.010	1.583	< 0.001
Territory Quality	1	0.005	0.813	0.982

776 Note: Significant (p < 0.05) predictors are shown in bold.

777

778 Table 3. A linear mixed effect model investigating variation in gut microbiome functional
 779 diversity (observed richness and Shannon diversity) in relation to within- (delta) and
 780 between- (mean) individual age in Seychelles warblers (n = 152 samples, 90 individuals).
 781 Functional diversity is based on eggNOG annotations. Observed richness and Shannon
 782 diversity were transformed using a scaled exponential and exponential function,
 783 respectively. Conditional R² = 35.6% and 13.7% respectively. Reference categories for
 784 categorical variables are shown in brackets

Observed Richness					
Predictor	Estimate	SE	df	t	P
(Intercept)	0.99	0.17	124.77	5.68	< 0.001
Delta Age	-0.12	0.04	137.00	-3.31	0.001
Mean Age	-0.03	0.01	89.42	-1.97	0.052
Terminal Year Bird (yes)	0.01	0.08	83.34	0.17	0.870
Season (winter)	-0.06	0.10	136.94	-0.64	0.525
Sex (female)	-0.06	0.08	81.33	-0.79	0.430
Days at 4°C	-0.19	0.09	127.35	-2.23	0.028
Time of day	-0.07	0.08	137.00	-0.88	0.381
Territory quality	-0.07	0.08	129.62	-0.88	0.381
Sample Year (2017)					
2018	0.13	0.15	135.76	0.82	0.416
2019	0.08	0.18	135.88	0.46	0.647
2020	0.36	0.20	136.54	1.82	0.071
2021	0.39	0.19	136.94	2.04	0.044
2022	0.56	0.19	128.48	2.90	0.004
2023	0.57	0.23	122.81	2.50	0.014
Random					
Individual ID	152 observations	90 individuals	Variance		0.050
Shannon Diversity					
Predictor	Estimate	SE	df	t	P
(Intercept)	757.59	182.06	119.47	4.16	< 0.001
Delta Age	-117.01	41.06	135.71	-2.85	0.005
Mean Age	-27.30	13.54	83.56	-2.02	0.047
Terminal Year Bird (yes)	17.93	79.75	76.74	0.23	0.823
Season (winter)	173.07	104.67	127.74	1.65	0.101
Sex (female)	-4.98	80.46	69.67	-0.06	0.951
Days at 4°C	-48.55	95.70	133.26	-0.51	0.613
Time of day	-21.18	81.57	132.14	-0.26	0.796
Territory quality	-0.74	85.97	136.99	-0.01	0.993
Sample Year (2017)					
2018	88.02	168.08	136.67	0.52	0.601
2019	32.22	200.48	136.71	0.16	0.873
2020	169.50	210.62	131.73	0.81	0.422
2021	464.12	206.85	136.39	2.24	0.026
2022	484.95	202.78	124.82	2.39	0.018
2023	453.37	238.55	116.14	1.90	0.060
Random					

Individual ID	152 observations	90 individuals	Variance	5046
---------------	------------------	----------------	----------	------

785 *Note:* Significant ($p < 0.05$) predictors are shown in bold.

786

787

788 Table 4. A PERMANOVA analysis of gut microbiome functional composition in relation to
789 age (and other factors) in the Seychelles warbler. The PERMANOVA was performed using
790 a Euclidean distance matrix calculated using CLR-transformed (eggNOG) abundances. N
791 = 153 samples. 91 individuals. Bird ID was included as a blocking factor.

Predictor	df	R ²	F	P
Age	1	0.007	1.096	0.044
Terminal Year	1	0.006	0.890	0.292
Season	1	0.011	1.823	0.042
Sample Year	6	0.052	1.374	0.020
Sex	1	0.008	1.250	0.001
Days at 4°C	1	0.010	1.569	0.007
Time of day	1	0.008	1.200	0.139
Territory quality	1	0.007	1.094	0.413

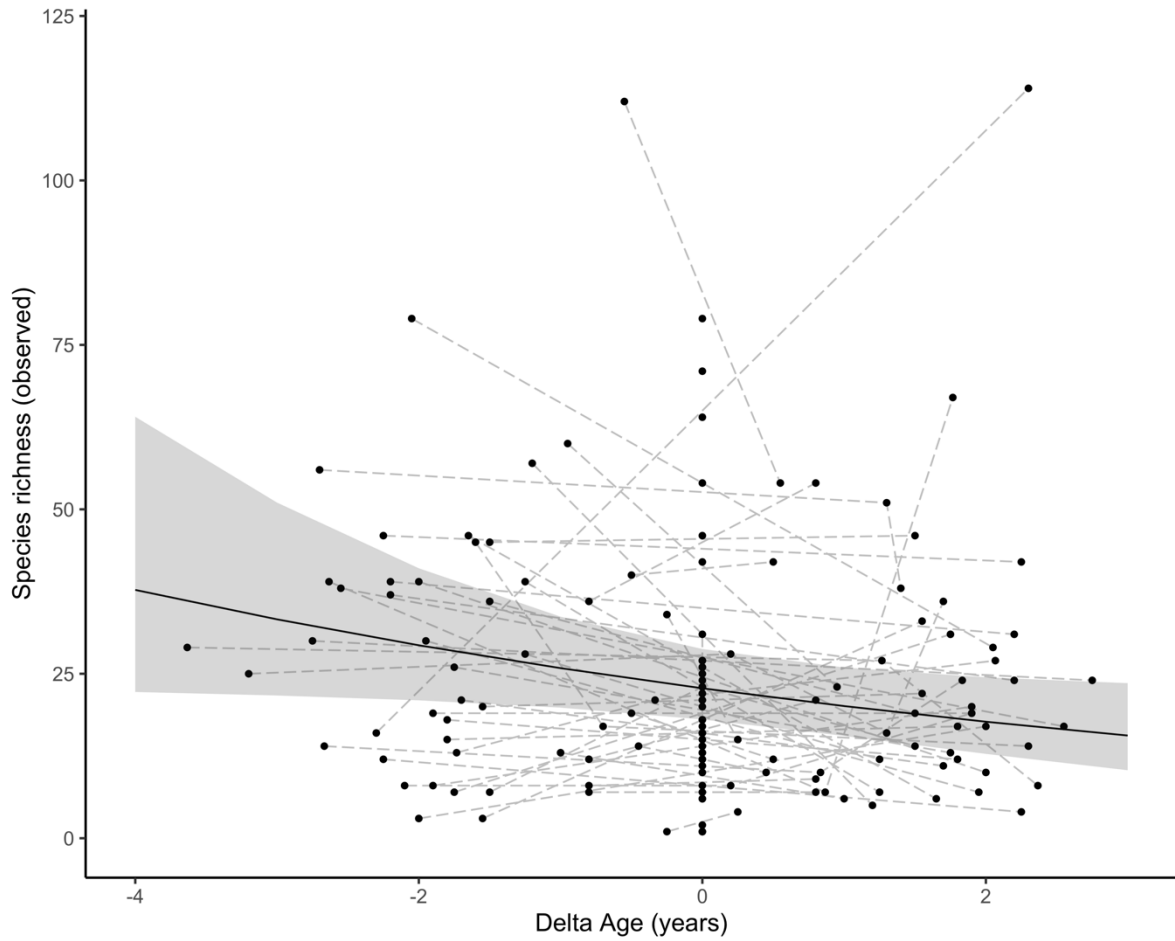
792 *Note:* Significant ($p < 0.05$) predictors are shown in bold.

793

794

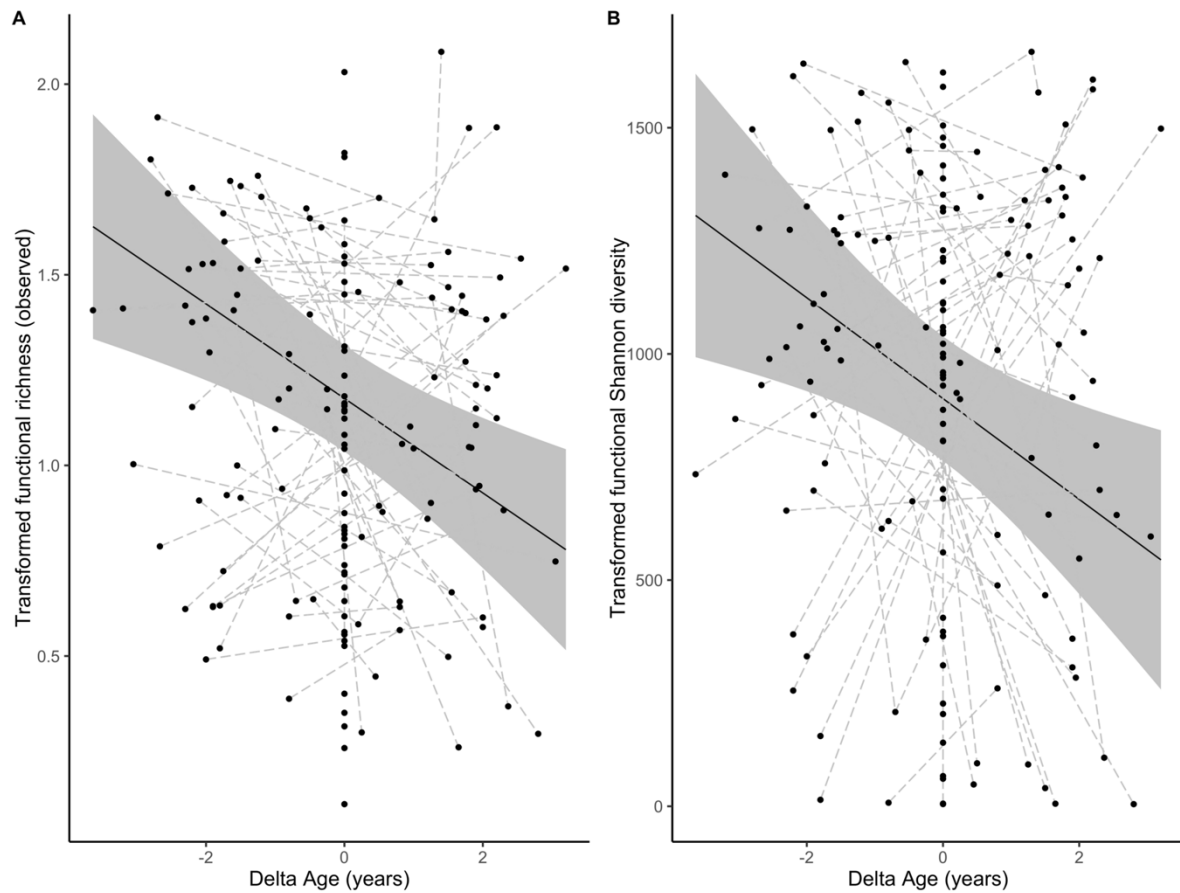
795 **Figures**

796



797
 798
 799
 800
 801
 802
 803
 804

Figure 1. Gut microbiome species richness in relation to within-individual, longitudinal differences in age (delta age in years) in Seychelles warblers. The solid line represents model predictions with 95% confidence intervals calculated from the generalised linear mixed effect model (Table 1). Each point represents an individual gut microbiome sample, and the dashed grey lines connect samples from the same individual (n = 151 samples, 91 individuals).



805

806 Figure 2. Gut microbiome functional diversity measured as (A) observed richness and (B)

807 Shannon diversity in relation to within-individual host age (years). Functional diversity

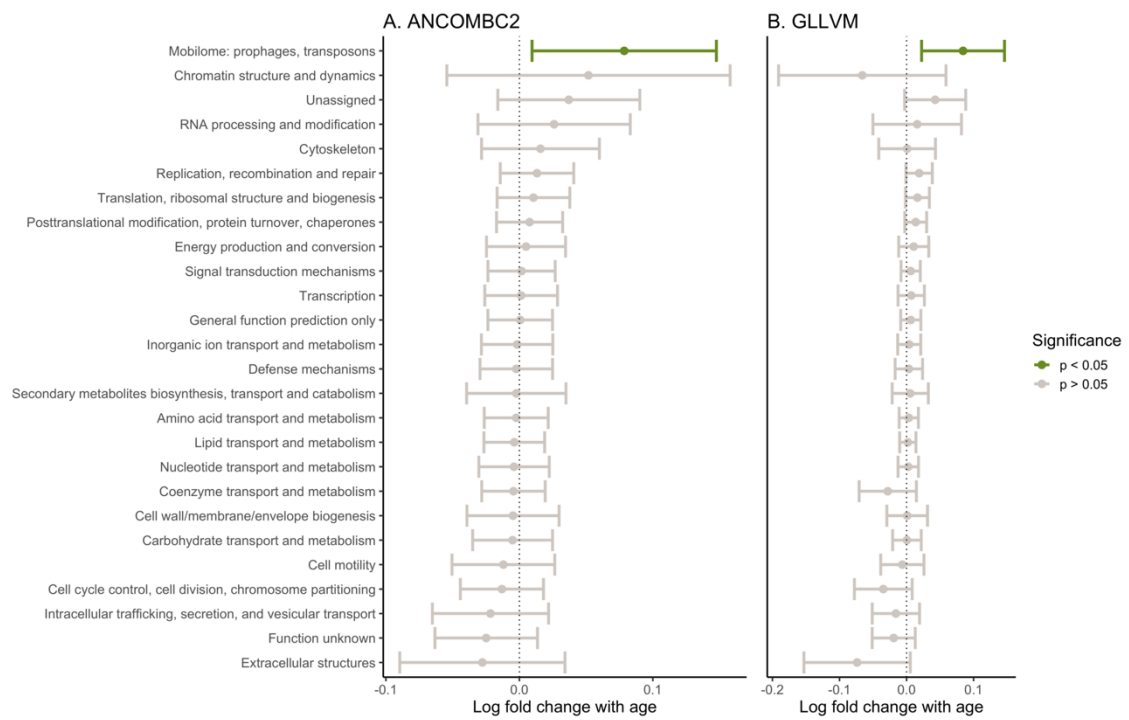
808 calculations are based on eggNOG orthologue groups. Solid lines represent model

809 predictions (\pm 95% confidence interval) from linear mixed effects models. Each point

810 represents a unique gut microbiome sample, and the dashed grey lines connect samples

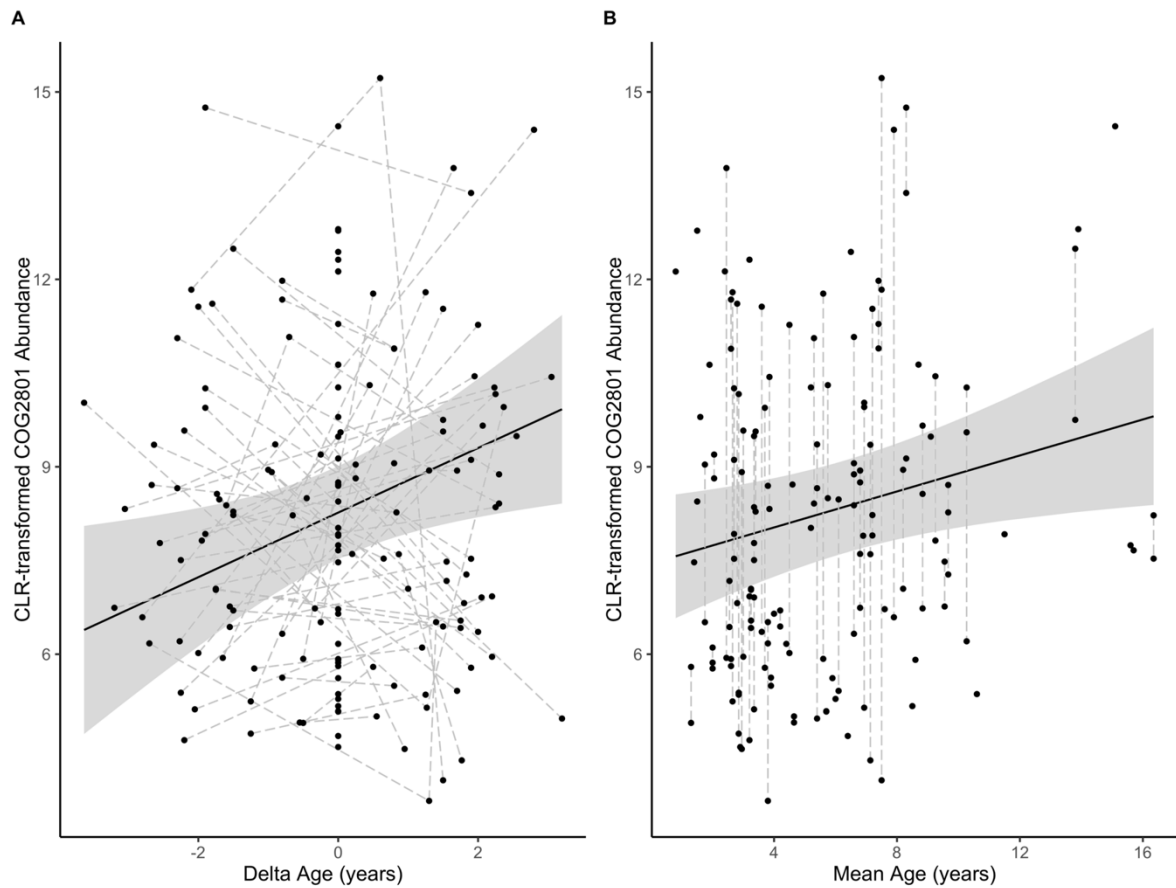
811 collected from the same individual (n = 152 samples, 90 individuals).

812



813
 814
 815
 816
 817
 818

Figure 3. Differential abundance analysis of functional gut microbiome cluster of orthologous genes (COG) categories in Seychelles warblers using (A) ANCOMBC2 and (B) GLLVM. Each COG category is represented on the y-axis. Points and error bars are coloured according to significance (green: $p < 0.05$; grey: $p > 0.05$).



819
 820 Figure 4. CLR-transformed COG2801 abundance in relation to (A) within-individual (delta)
 821 host age and (B) between-individual (mean) host age in the gut microbiome of Seychelles
 822 warblers. The solid line represents model predictions (\pm 95% confidence intervals) from a
 823 linear mixed effect model (Table 5). Each point represents a gut microbiome sample with
 824 dashed grey lines connecting samples from the same individual (n = 153 samples, 91
 825 individuals).
 826

827 **Acknowledgements**

828 We thank Nature Seychelles for facilitating fieldwork on Cousin Island and the Seychelles
829 Bureau of Standards and the Ministry of Agriculture, Climate Change & Environment for
830 providing permission to conduct fieldwork and sample collection. This study would not
831 have been possible without the contribution of exceptional fieldworkers, laboratory
832 technicians and database managers associated with the Seychelles Warbler Project. The
833 research presented in this paper was carried out on the High-Performance Computing
834 Cluster supported by the Research and Specialist Computing Support service at the
835 University of East Anglia.

836

837 **Compliance with ethical standards**

838 **Ethics Statement**

839 Fieldwork was carried out in accordance with local ethical regulations and agreements
840 (UEA ethics approval ID ETH2223-0665). The Seychelles Department of Environment
841 and the Seychelles Bureau of Standards approved the fieldwork (permit number A0157).

842

843 **Conflict of interest**

844 The authors declare that they have no conflict of interest.

845

846 **Data availability statement**

847 All raw sequence data have been submitted to the European Nucleotide Archive (ENA)
848 database under the study accession number PRJEB81709.

849

850 **Code availability statement**

851 The data files and script necessary to reproduce the statistical analysis and plots are
852 provided at https://github.com/Chuen-Lee/SW_Senescence_GM

853

854 **Supplementary Information:**

855

856 **Gut microbiome composition and function – including**
857 **transposase gene abundance - varies with age, but not**
858 **senescence, in a wild vertebrate**

859

860 Wild gut microbiome changes with age

861

862 Chuen Zhang Lee^{1*}, Sarah F. Worsley¹, Charli S. Davies¹, Ece Silan², Terry Burke³,
863 Jan Komdeur⁴, Falk Hildebrand², Hannah L. Dugdale⁴, David S. Richardson^{1,5*}

864

865

866 ¹ School of Biological Sciences, University of East Anglia, Norfolk, UK

867 ² Quadram Institute, Norwich Research Park, Norfolk, UK

868 ³ Ecology and Evolutionary Biology, School of Biosciences, University of Sheffield,
869 Sheffield, UK

870 ⁴ Groningen Institute for Evolutionary Life Sciences (GELIFES), University of Groningen,
871 Groningen, The Netherlands

872 ⁵ Nature Seychelles, Roche Caiman, Mahé, Republic of Seychelles

873

874 *Correspondence: david.richardson@uea.ac.uk, chuen.lee@uea.ac.uk

875

876 **Supplementary methods**

877 Sample collection and storage

878 Between 2017 and 2023 all caught birds were placed in a disposable flat-bottom waxed
879 paper bag containing a sterilised plastic weighing tray underneath a sterilised metal grate
880 [43,55,100]. This allows the bird to stand on the grate and faecal samples to fall into the
881 sterile tray, minimising contact with the bird's surface. After ca 15 minutes (or when
882 defecation was observed) the bird was removed. Any sample was collected, using a
883 single-use sterile flocked swab, and placed into a microcentrifuge tube containing 1 mL of
884 absolute ethanol. Samples were stored at 4°C in the field before being transferred to -
885 80°C for long-term storage.

886

887 Bioinformatics

888 Briefly, host reads were removed by mapping sequences to the Seychelles warbler
889 genome (unpublished; complete BUSCO = 96.0% with a total length = 1,081,018,985 bp),
890 using Kraken 2 (version 2.1.3). Remaining reads underwent quality filtering using sdm
891 software version 2.14 beta [101,102]. After trimming, two samples and five hand controls
892 were removed because they did not return enough reads for subsequent analysis (<
893 300,000 reads). An average of 20,481,040 ($\pm 1,109,059$ SE) paired-end reads per sample
894 were retained across the remaining samples.

895

896 The same trimmed reads were also used for *de novo* metagenome assembly, as
897 implemented in MATAFILER: MEGAHIT version 1.2.9 [103] was used for metagenomic
898 assemblies, on these genes were predicted using Prodigal version 2.6.3 [104] and
899 clustered into a gene catalogue (95 % identity) of 19,527,109 gene clusters, and a gene
900 abundance matrix created using rtk2 [105]. Functional annotations of clustered genes
901 were done using eggNOGmapper version 2.1.12 and the evolutionary genealogy of genes:
902 Non-supervised Orthologous Groups (eggNOG) database version 4 [82,106].
903 Subsequently, genome binning was done with SemiBin which created 4,176 bins (mean
904 completeness = 34.95%, mean contamination = 1.41%) [107]. The bins were then filtered
905 based on >80% completeness and <5% contamination using CheckM2 [108]; this
906 retained 824 metagenome-assembled genomes (MAGs). MAGs were dereplicated across
907 samples to generate 323 non-redundant metagenomic species (MGS) level bins, using
908 clusterMAGs (<https://github.com/hildebra/clusterMAGs>). For MGSs, taxonomic
909 assignment was performed using a marker-based approach with GTDB database version
910 214 [109]. Due to the high individuality of the warbler GM and the high sequencing
911 coverage required to assign MGS, only one MGS was present in more than 50% of
912 sequenced samples and relatively fewer MGSs were identified per sample (average $17 \pm$
913 1.3 SE per sample) which is likely to be an underestimate of the true diversity of the GM.

914

915 Therefore, Metaphlan4 version 4.1.0 (which is assembly-free and therefore requires lower
916 coverage) was used to taxonomically classify reads using the default parameters [110].
917 Metaphlan4 assignments identified an average of 29.3 ± 2.0 species genome bins per

918 sample and were used for the subsequent taxonomic analysis and MGS was only used for
919 tracking functional annotations back to their taxonomy.

920

921 Post-hoc functional differential abundance analysis

922 Posthoc investigations were performed on individual eggNOG members found within the
923 COG categories that were significantly differentially abundant with age. Firstly, a linear
924 model was performed for each significant eggNOG member to test whether age-related
925 changes were driven by between- or within-individual processes. Second, we tested if
926 changes in the abundance of significant eggNOG members could be driven by changes in
927 the abundance of the taxa from which these genes originate. To test this, the total
928 abundance of MGSs carrying the eggNOG gene orthologs of interest was used as the
929 response variable and age was included as a predictor in a lmer model. Furthermore,
930 genera of eggNOG-carrying MGSs were matched with metaphlan4 genera to test whether
931 the total abundance of known eggNOG-carrying genera was significantly associated with
932 host age. Lastly, a protein-protein Basic Local Alignment Search Tool (BLASTp) analysis of
933 each eggNOG gene ortholog of interest embedded within each MGS was performed to
934 determine the identity of genes [111,112]. To test if the differential abundance of eggNOG
935 members was driven by changes in the abundance of a specific gene (versus the
936 cumulative abundance of many genes), gene catalogues assigned to the eggNOG cluster
937 of interest (filtered to those with > 20% prevalence and 0.1% detection) were tested for
938 differential abundance.

939

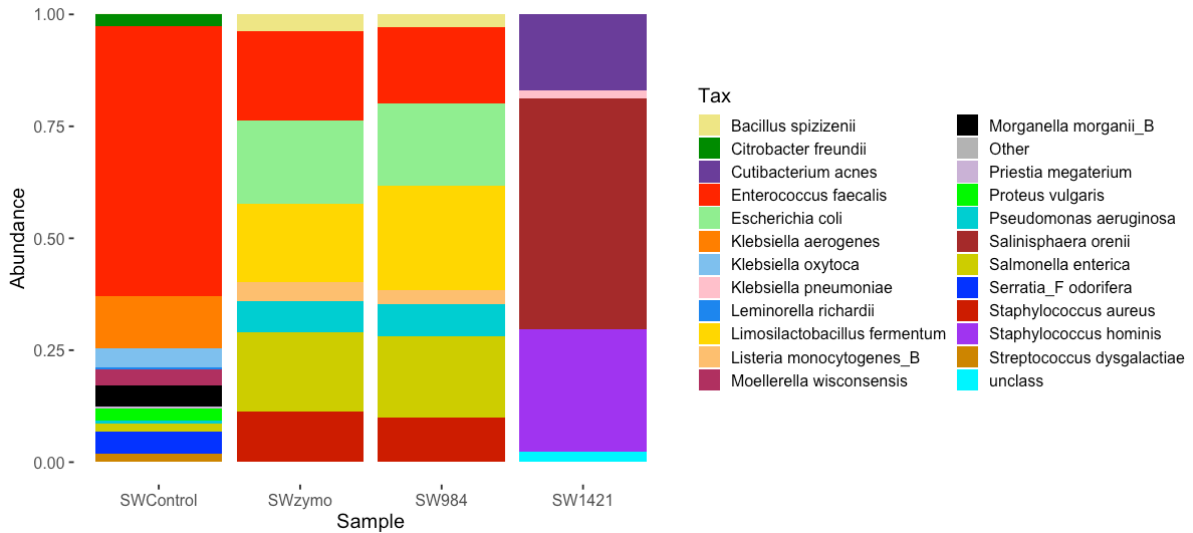
940

941 **Supplementary Figures and Tables**

942 Components of positive controls were successfully recovered as high-quality MGSs in
943 acceptable relative abundances (Figure S2). Only 2 out of the 18 MGS from controls were
944 found in faecal samples, both were widespread species *Enterococcus faecalis* and
945 *Klebsiella pneumoniae* [113,114]. *E. faecalis* was part of the positive control but not found
946 in the hand controls. *K. pneumoniae* was found in hand controls as well as samples but due
947 to the low abundance in hand controls, we decided to retain all species for taxonomic
948 analysis.

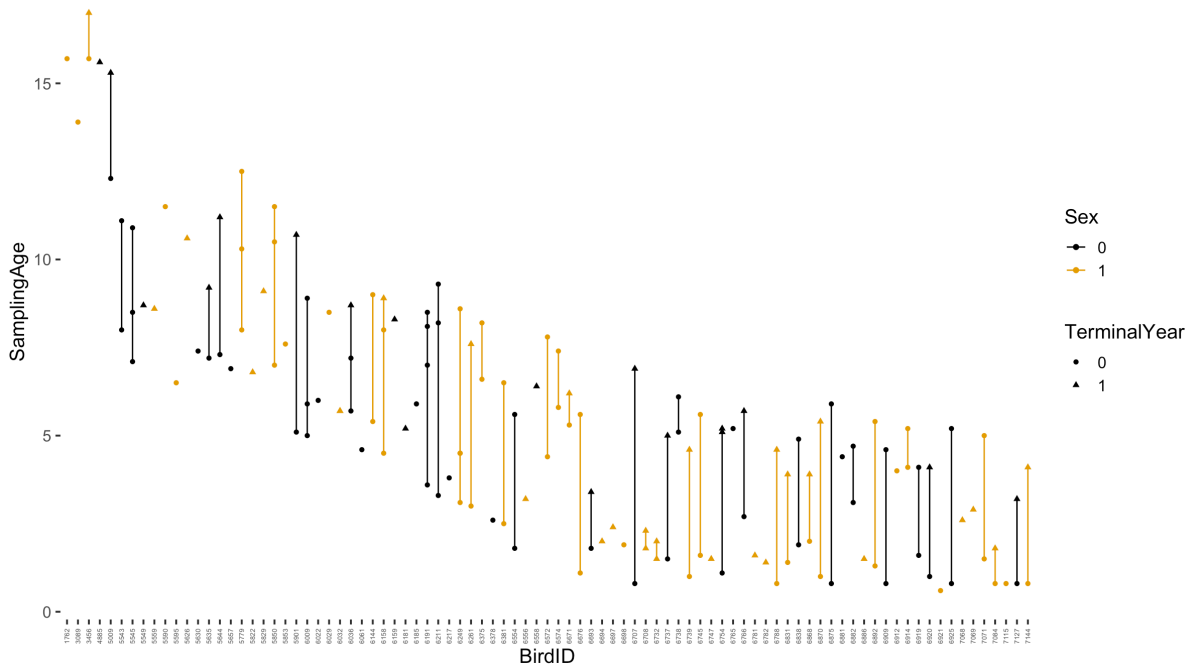
949

950



951
952
953
954
955
956
957
958
959
960
961

Figure S1. Controls and relative abundance of MGS at the species level. SWControl is positive control (ZymoBIOMICS Fecal Reference with TruMatrix™ Technology), SW984 and SWzymo are positive controls (ZymoBIOMICS Microbial Community Standard) sequenced separately, and SW1421 is a contamination (hand) control from 2023. We identified subspecies of *Bacillus subtilis* - *Bacillus spizizenii* and *Lactobacillus fermentum* - *Limosilactobacillus fermentum*. In SW1421 hand control, *Cutibacterium acnes* is linked to acne, *Klebsiella pneumoniae* is commonly found in the gut, *Salinisphaera orenii* are bacteria commonly isolated in high salinity environments, *Staphylococcus hominis* is commonly found to be harmless on human and animal skin.



962
963
964
965

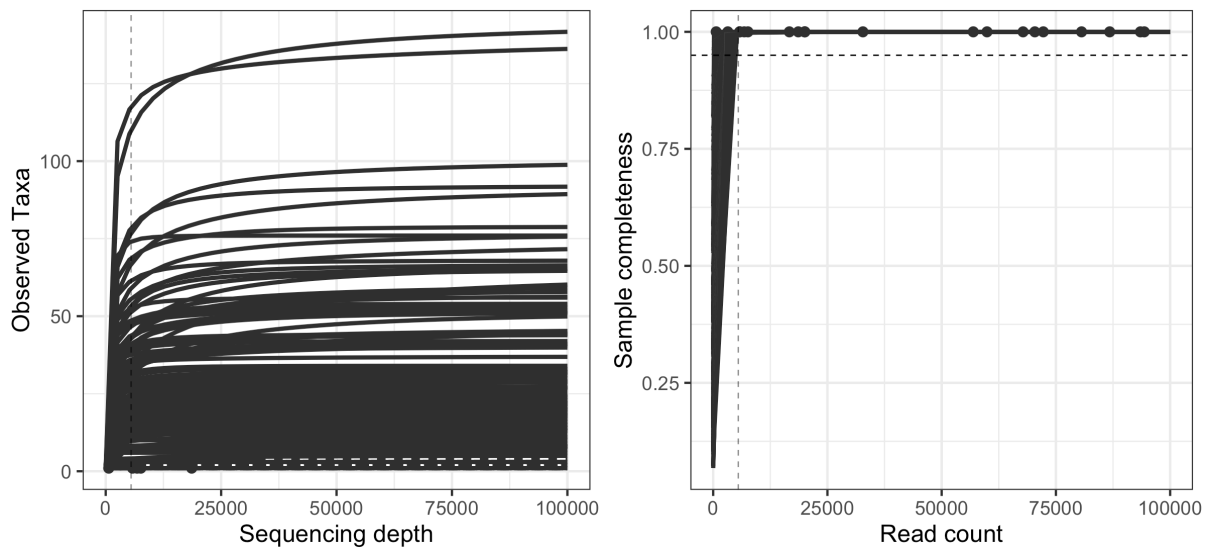
Figure S2. Seychelles warbler gut microbiome samples that were retained for analysis after sequencing and bioinformatics (n = 153 from 91 individuals). Points represent each sample, the y-axis represents individual's age at sampling, whilst the x-axis represents

966 individuals. Solid lines connect samples that were collected from the same individual.
 967 Colours represent the different sex (black = female, gold = male). Shape represents
 968 whether the sample was collected in the individual's terminal year (circle = no, triangle =
 969 yes).

970

971

972 **Taxonomy**



973

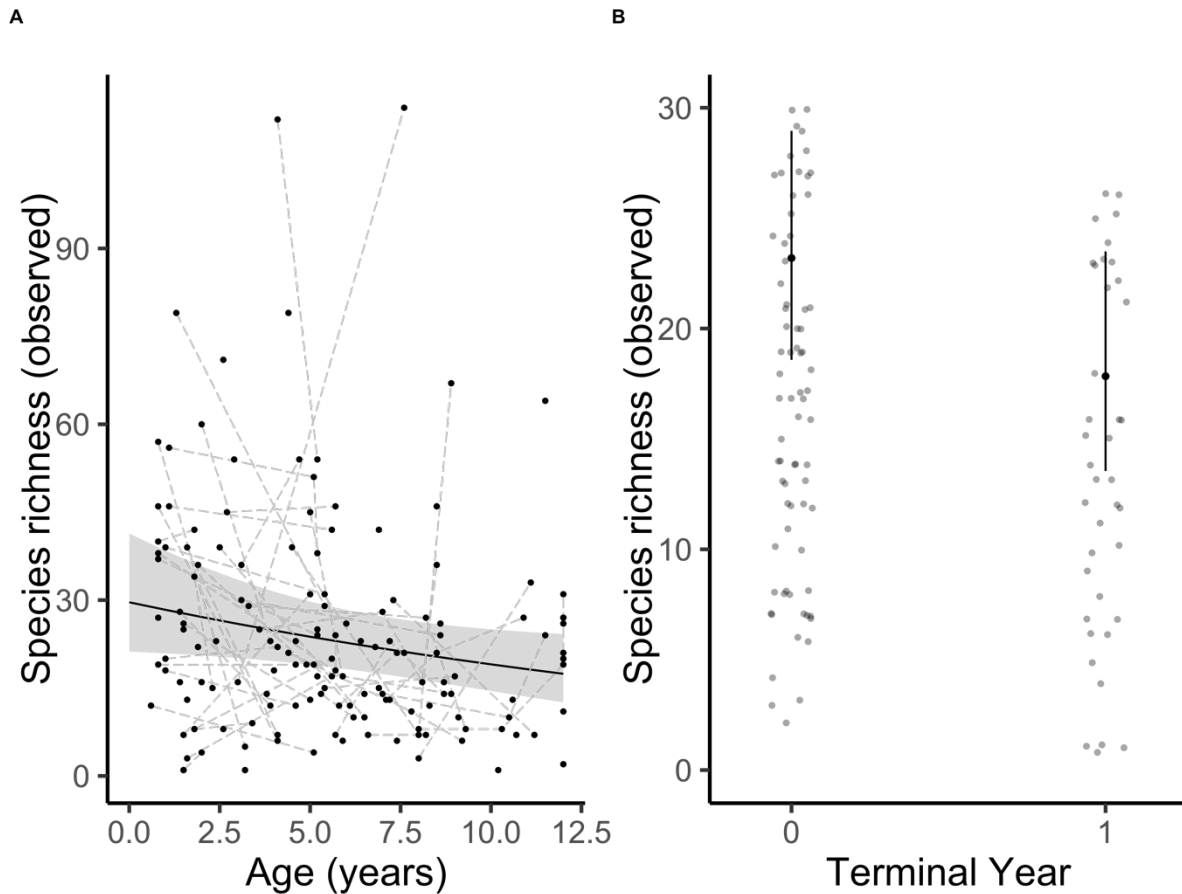
974 Figure S3. Sequencing depth against number of observed (metaphlan4) assembly-free
 975 taxonomic assignments (left) and read count against sample completeness (right) of each
 976 gut microbiome sample from Seychelles warblers (n = 153). 5500 reads at 95%
 977 completeness.

978

979 Table S1. A generalised linear mixed effect model with a negative binomial distribution
 980 investigating the relationship between age, terminal year, and species richness in the gut
 981 microbiome of Seychelles warblers (n = 151 samples, 91 individuals). Significant (p < 0.05)
 982 predictors are shown in bold. Conditional R² = 38.9%.

Predictor	Estimate	SE	z	P
(Intercept)	-125.20	71.62	-1.75	0.081
Age	-0.04	0.02	-2.10	0.036
Terminal Year (yes)	-0.26	0.13	-2.06	0.039
Season (winter)	0.01	0.13	0.09	0.932
Sex (female)	0.01	0.13	0.05	0.959
Time at 4°C	-0.18	0.14	-1.33	0.183
Time of day	0.22	0.12	1.82	0.069
Territory quality	-0.08	0.12	-0.67	0.506
Sample Year	0.06	0.04	1.79	0.073
Random				
Individual ID	151 observations	91 individuals	Variance	0.14

983



984
 985 Figure S4. Species richness prediction from glmer.nb of the gut microbiome in the
 986 Seychelles warblers (n = 151 samples from 91 individuals). (A) Species richness against
 987 host age in years, solid black line and grey shaded area represent model predictions and
 988 confidence intervals respectively, points represent raw data. (B) Species richness against
 989 terminal year (0: No, 1: Yes), black dot and lines represent model predictions and error bars
 990 respectively, grey dots represent raw data points.

991
 992 Table S2. A linear mixed effect model of Shannon diversity with chronological age and
 993 terminal year in the gut microbiome of Seychelles warblers (n = 151 samples, 91
 994 individuals). Significant ($p < 0.05$) predictors are shown in bold. Conditional $R^2 = 46.4\%$.

Predictor	Estimate	SE	df	t	P
(Intercept)	-152.40	76.85	142.00	-1.98	0.049
Age	-0.01	0.02	86.36	-0.46	0.644
Terminal Year (yes)	-0.16	0.14	133.79	-1.17	0.244
Season (winter)	-0.12	0.17	130.60	-0.69	0.491
Sex (female)	0.10	0.16	74.64	0.63	0.529
Time at 4°C	-0.32	0.15	113.36	-2.15	0.034
Time of day	-0.01	0.13	133.62	-0.10	0.920
Territory quality	-0.14	0.14	124.33	-1.02	0.311
Sample Year	0.08	0.04	142.00	2.00	0.047
Random					

Individual ID	151 observations	91 individuals	Variance	0.27
---------------	------------------	----------------	----------	------

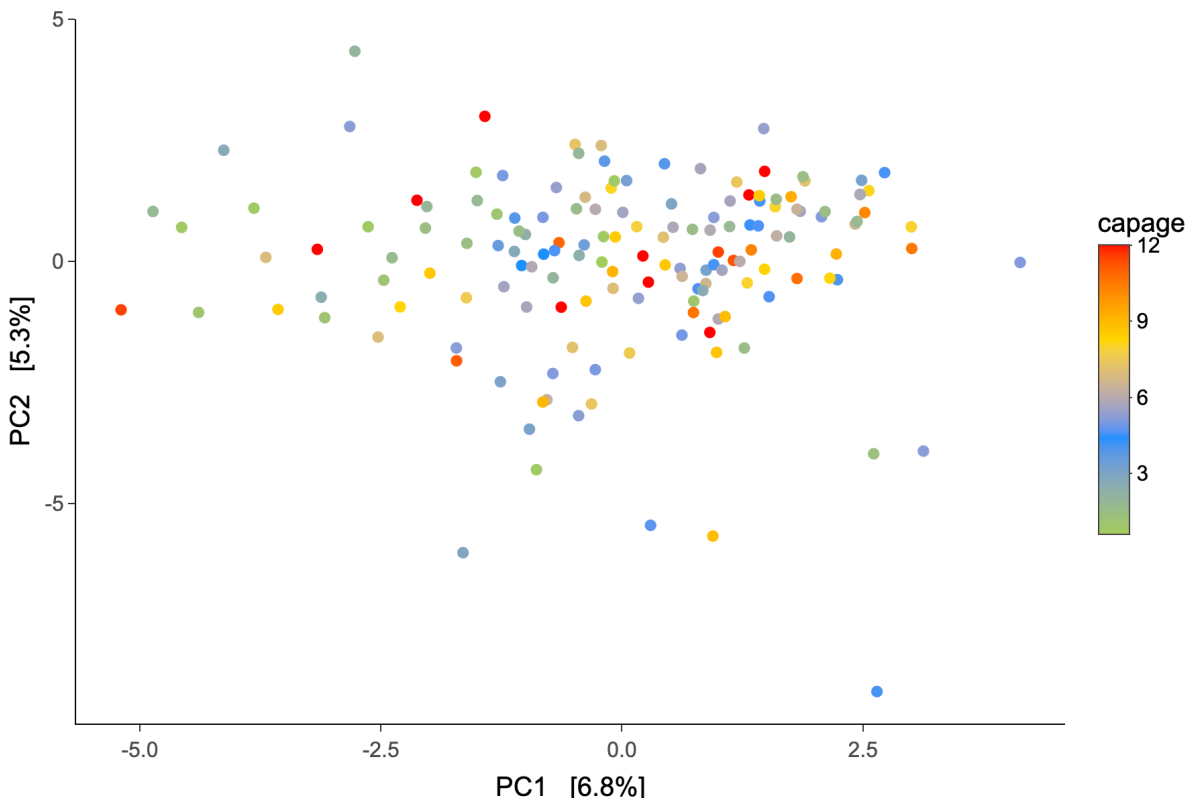
995

996 Table S3. A linear mixed effect model of Shannon diversity within- and between- individual
 997 age analysis, accounting for subsequent close-to-death samples in the gut microbiome of
 998 Seychelles warblers (n = 151 samples, 91 individuals). Significant (p < 0.05) predictors are
 999 shown in bold. Conditional R² = 49.7%.

Predictor	Estimate	SE	df	z	P
(Intercept)	0.95	0.35	129.65	2.75	0.007
Delta Age	-0.07	0.07	135.41	-1.12	0.265
Mean Age	-0.18	0.16	77.16	-1.14	0.257
Terminal Year Bird (yes)	-0.01	0.03	81.30	-0.24	0.809
Sample Year	0.09	0.06	105.90	1.60	0.11
Season (winter)	-0.12	0.17	128.97	-0.72	0.470
Sex (female)	0.10	0.16	75.58	0.62	0.535
Time at 4°C	-0.33	0.15	112.75	-2.24	0.027
Time of day	-0.02	0.13	131.47	-0.12	0.908
Territory quality	-0.15	0.14	122.92	-1.08	0.281
Random					
Individual ID	151 observations	91 individuals	Variance	0.3003	

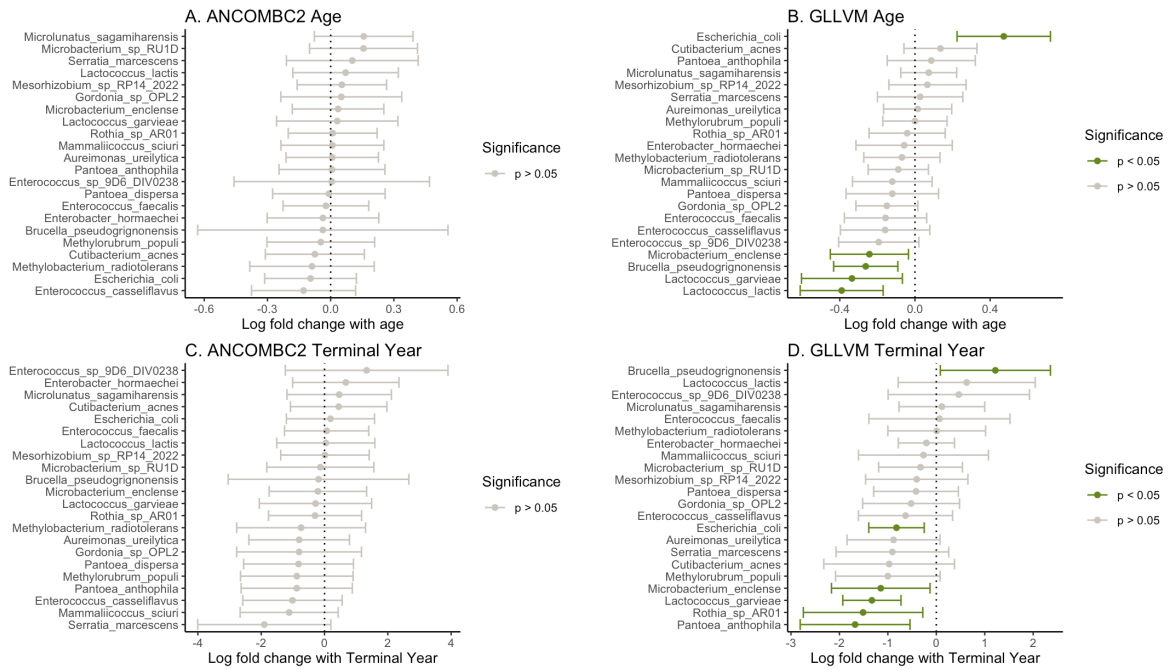
1000

1001



1002

1003 Figure S5. PCA plot of CLR-transformed reads in Euclidean distance, coloured by age.



1004
 1005
 1006
 1007
 1008
 1009

Figure S6. Taxonomic differential abundance analysis for common species (> 20% prevalence in the population). (A) ANCOMBC2 with age, (B) GLLVM with age, (C) ANCOMBC2 with terminal year, (D) GLLVM with terminal year. Significant ($p < 0.05$). Green = significant ($p < 0.05$) log fold change, grey = insignificant log fold change.

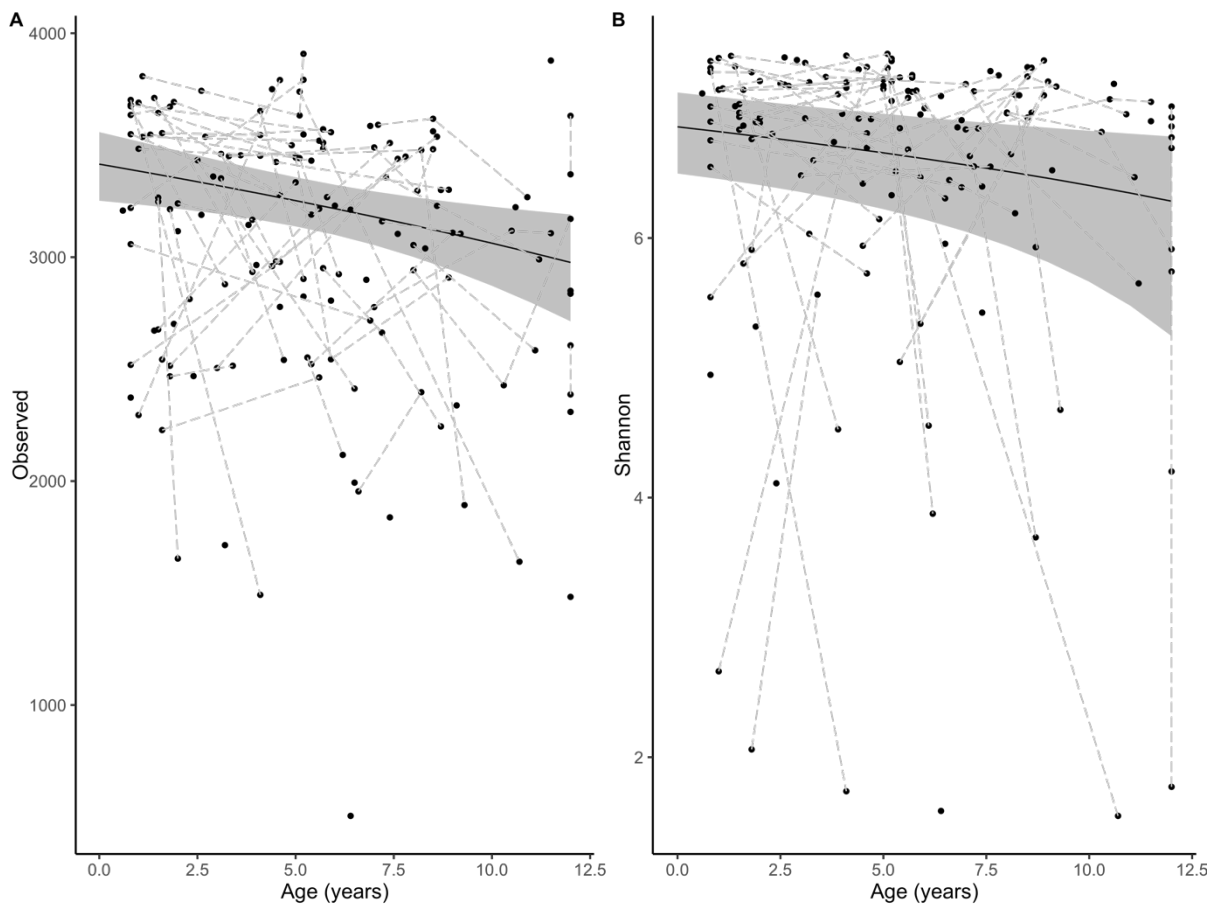
1010
 1011
 1012
 1013

Table S4. A linear mixed effect model testing for age-related changes in functional scaled exponentially transformed observed richness and exponentially transformed Shannon diversity of eggNOG annotations in the gut microbiome of Seychelles warblers ($n = 152$ samples, 90 individuals). Conditional $R^2 = 33.7\%$ and 9.2% respectively.

Observed Richness						
Predictor	Estimate	SE	df	t	P	
(Intercept)	-109.417	42.293	142.715	-2.587	0.011	
Age (years)	-0.036	0.013	92.620	-2.877	0.005	
Terminal Year (yes)	-0.124	0.077	142.784	-1.605	0.111	
Season (winter)	-0.080	0.078	141.089	-1.024	0.307	
Sex (female)	-0.080	0.080	78.890	-1.008	0.317	
Days at 4°C	-0.198	0.082	130.818	-2.422	0.017	
Time of day	-0.027	0.071	142.930	-0.373	0.710	
Territory quality	-0.074	0.072	134.361	-1.030	0.305	
Sample Year	0.055	0.021	142.686	2.618	0.010	
Random						
Individual ID	152 observations	90 individuals	Variance	0.047		
Shannon Diversity						
Predictor	Estimate	SE	df	t	P	
(Intercept)	-92473.06	46119.45	143.00	-2.01	0.047	

Age (years)	-31.31	12.59	143.00	-2.49	0.014
Terminal Year (yes)	-20.41	83.74	143.00	-0.24	0.808
Season (winter)	105.32	85.76	143.00	1.23	0.221
Sex (female)	-21.32	78.14	143.00	-0.27	0.785
Time at 4°C	-36.85	92.11	143.00	-0.40	0.690
Time of day	27.32	76.97	143.00	0.36	0.723
Territory quality	-1.21	79.70	143.00	-0.02	0.988
Sample Year	46.31	22.85	143.00	2.03	0.045
Random					
Individual ID	152 observations	90 individuals	Variance		108.9

1014



1015

1016

1017

1018

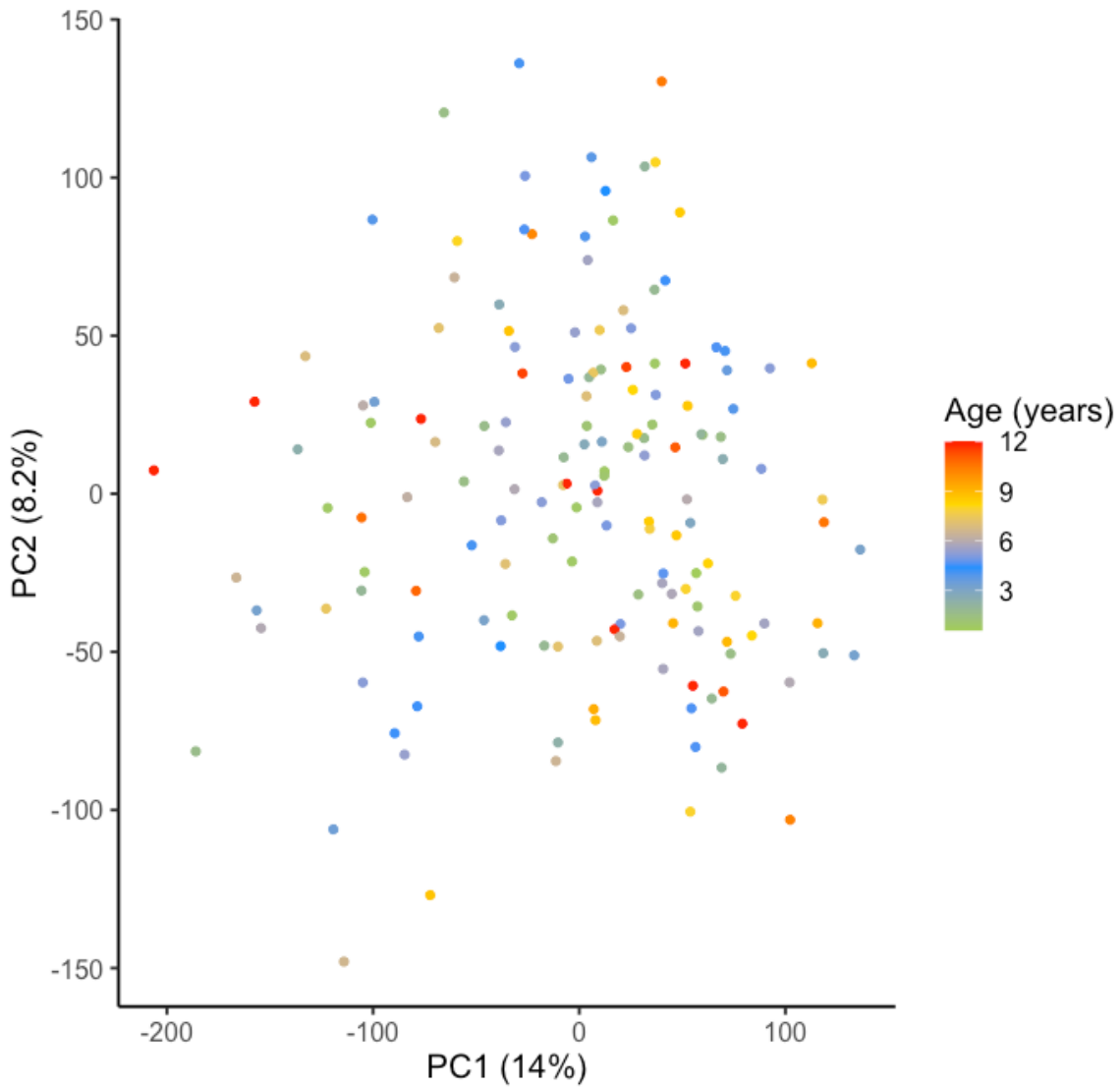
1019

1020

1021

1022

Figure S7. Evolutionary genealogy of genes: Non-supervised Orthologous Groups (eggNOG) (A) observed richness and (B) Shannon diversity against host age (years) model prediction from linear mixed effect model in the gut microbiome of Seychelles warblers. The solid line represents model predictions and ribbon-shading represent confidence intervals from model predictions. Each point represents a sample, and the dashed grey lines connect samples collected from the same individual (n = 152 samples from 90 individuals).



1023
 1024
 1025
 1026

Figure S8. Functional PCA plot of CLR-count, euclidean distances of eggNOG annotations

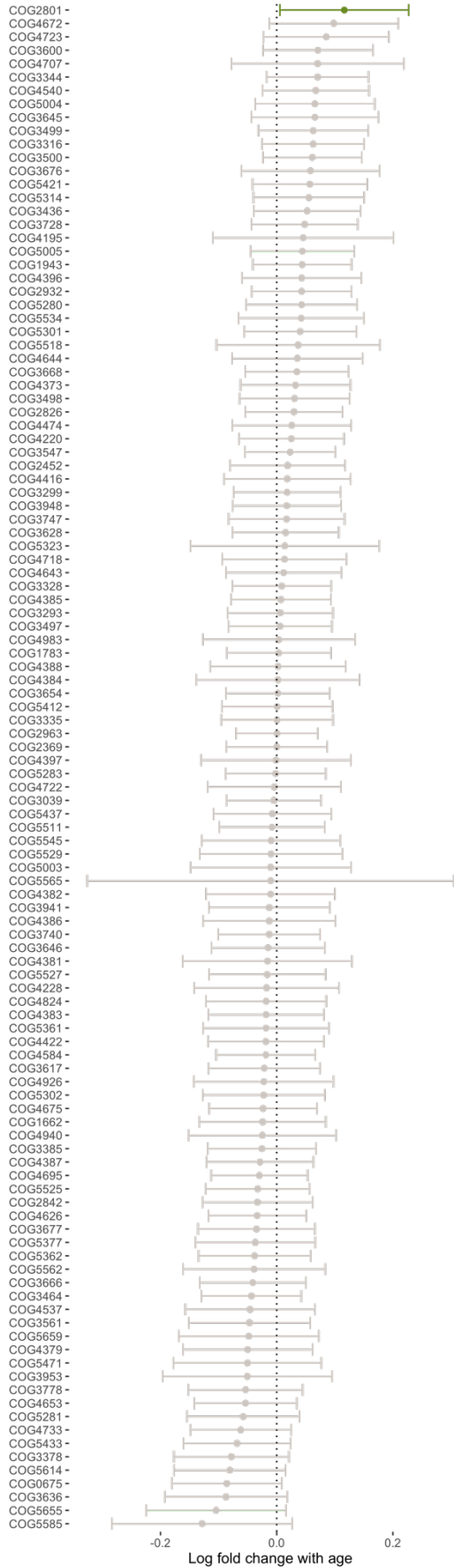
Table S5. COG functional categories [71]

Abbreviation	COG Functional Categories
A	RNA processing and modification
K	Transcription
L	Replication, recombination and repair
B	Chromatin structure and dynamics
D	Cell cycle control, cell division, chromosome partitioning
V	Defense mechanisms
Y	Nuclear structure
T	Signal transduction mechanisms
M	Cell wall/membrane/envelope biogenesis
N	Cell motility
Z	Cytoskeleton
W	Extracellular structures

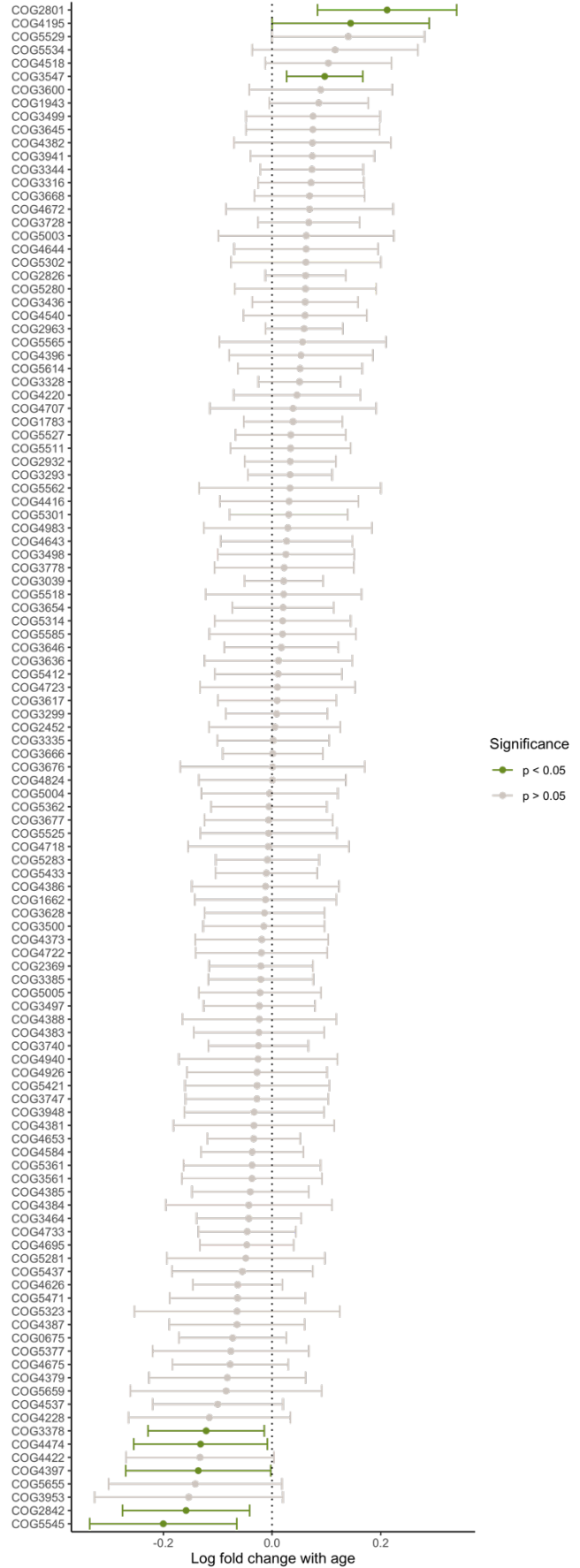
U	Intracellular trafficking, secretion, and vesicular transport
O	Posttranslational modification, protein turnover, chaperones
X	Mobilome: prophages, transposons
C	Energy production and conversion
G	Carbohydrate transport and metabolism
E	Amino acid transport and metabolism
F	Nucleotide transport and metabolism
H	Coenzyme transport and metabolism
I	Lipid transport and metabolism
P	Inorganic ion transport and metabolism
R	General function prediction only
Q	Secondary metabolites biosynthesis, transport and catabolism
S	Function unknown
`	Unassigned

1027

A. ANCOMBC2



B. GLLVM



1029 Figure S9 Differential abundance of COG X eggNOG members (A) ANCOMBC2 and (B)
 1030 GLLVM.

1031

1032 Table S7. A linear mixed effect model of COG2801 abundance in the gut microbiome of
 1033 Seychelles warblers in relation to within- (delta) and between- individual (mean) age. n =
 1034 153 samples, 91 individuals. Significant (p < 0.05) predictors in bold. Conditional R² =
 1035 14.7%. Reference categories for categorical variables are shown in brackets

Predictor	Estimate	SE	df	t	P
(Intercept)	9.700	0.971	115.370	9.989	< 0.001
Delta Age	0.549	0.218	141.991	2.516	0.013
Mean Age	0.157	0.062	85.606	2.534	0.013
Terminal Year Bird (yes)	0.028	0.420	69.803	0.067	0.947
Season (winter)	-0.502	0.553	132.368	-0.908	0.365
Sex (female)	0.219	0.422	63.434	0.520	0.605
Days at 4°C	-0.196	0.495	136.509	-0.396	0.693
Time of day	-0.313	0.428	136.421	-0.730	0.466
Territory quality	-0.315	0.452	141.901	-0.697	0.487
Sample Year (2017)					
2018	-1.662	0.902	140.921	-1.844	0.067
2019	-1.457	1.068	141.645	-1.363	0.175
2020	-2.200	1.129	134.384	-1.949	0.053
2021	-2.911	1.119	140.585	-2.601	0.010
2022	-3.341	1.098	118.243	-3.042	0.003
2023	-3.215	1.289	111.442	-2.495	0.014
Random					
Individual ID	153 observations	91 individuals		Variance	0.1776

1036

1037

1038 Table S8. BLASTp top hits for each COG2801 found in the genomes of all constructed
 1039 metagenomics species (MGS) from the gut microbiome of Seychelles warblers (n = 153
 1040 from 91 individuals).

Top hit (contains keyword)	Count	Percentage
IS3 transposase	154	30%
otherIS transposase	64	13%
transposase	170	33%
integrase	30	6%
Mobile element protein	4	1%
Helix-turn-helix	19	4%
Hypothetical protein	45	9%
Unknown	23	5%

1041

1042

1043 Table S9. Linear mixed model on the CLR-transformed abundance of metagenomic
 1044 species in the gut microbiome of Seychelles warblers (n = 2589 from 89 individuals). To
 1045 test if COG2801-carrying MGS significantly differed in abundance with host age.
 1046 Significant (p < 0.05) predictors are shown in bold. Conditional R² = 46.9%.

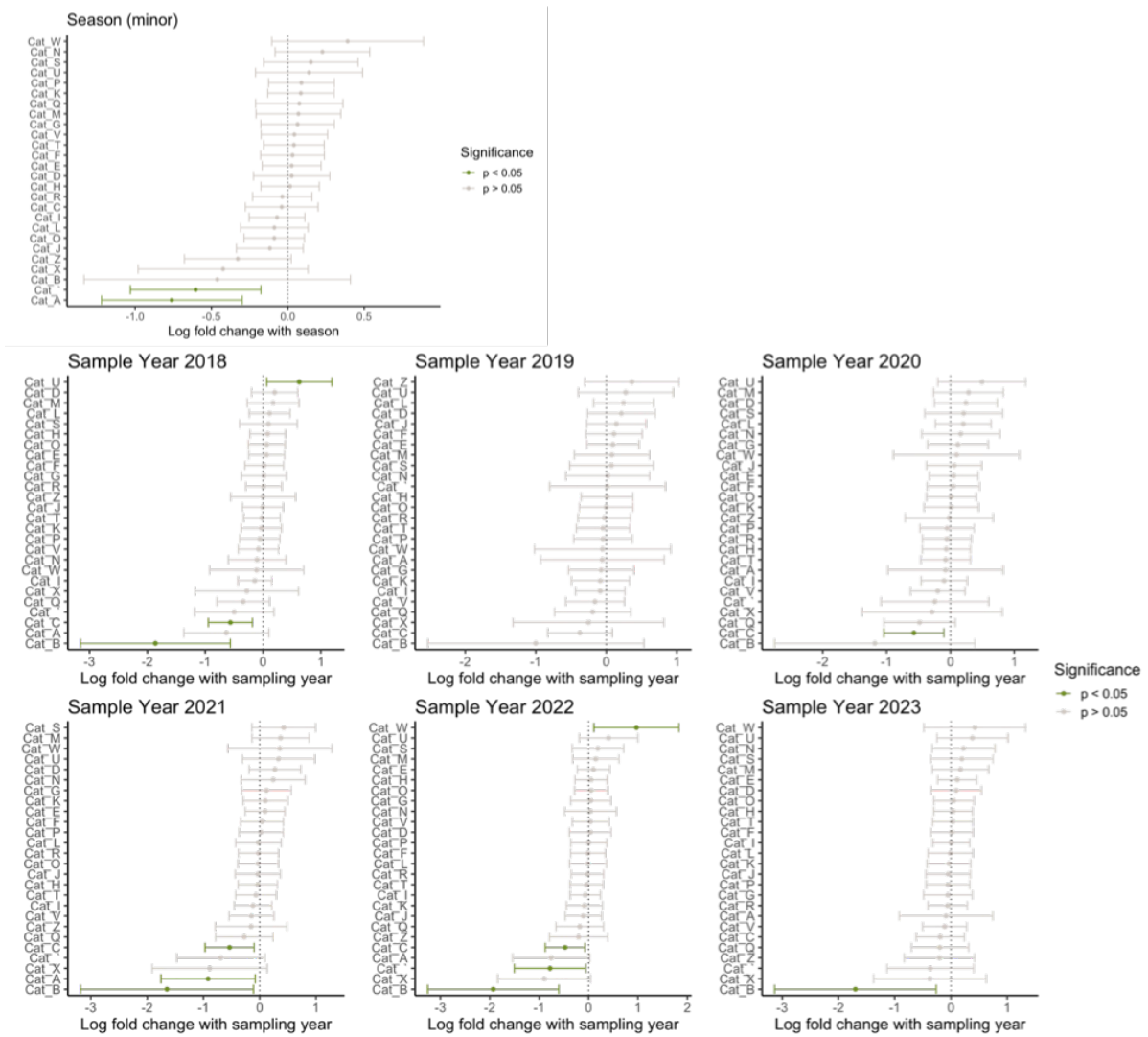
Predictor	Estimate	SE	df	t	P
(Intercept)	5.44	0.41	233.52	13.34	< 0.001
Age	0.03	0.04	69.32	0.79	0.432
Terminal Year (yes)	0.24	0.19	339.71	1.26	0.210
Season (winter)	-0.09	0.22	394.36	-0.43	0.671
Sex (female)	0.01	0.26	69.10	0.02	0.982
Time at 4°C	-0.44	0.18	434.74	-2.40	0.017
Time of day	-0.35	0.18	395.12	-2.01	0.045
Territory quality	-0.47	0.17	379.46	-2.85	0.005
Sample Year (2017)					
2018	-0.77	0.41	402.12	-1.90	0.059
2019	-1.69	0.46	416.15	-3.71	0.000
2020	-1.19	0.48	360.43	-2.50	0.013
2021	-0.70	0.46	334.48	-1.53	0.127
2022	-0.56	0.45	266.74	-1.25	0.213
2023	-0.65	0.49	239.09	-1.33	0.186
Random					
Individual ID	874 observations	85 individuals		Variance	1.042

1047
 1048 Table S10. Linear mixed model on the CLR-transformed abundance of metaphlan4 genera
 1049 in the gut microbiome of Seychelles warblers (n = 4477 from 91 individuals). To test if
 1050 known COG2801-carrying genera significantly differed in abundance with host age.
 1051 Significant (p < 0.05) predictors are shown in bold. Conditional R² = 16.8%.

Predictor	Estimate	SE	df	t	P
(Intercept)	9.08	0.45	316.13	20.37	< 0.001
Age	0.04	0.04	77.18	0.91	0.363
Terminal Year (yes)	0.30	0.22	272.48	1.37	0.173
Season (winter)	-0.30	0.27	271.10	-1.09	0.276
Sex (female)	0.15	0.27	70.01	0.54	0.589
Time at 4°C	-0.52	0.22	373.62	-2.34	0.020
Time of day	-0.60	0.21	224.79	-2.82	0.005
Territory quality	0.03	0.21	486.10	0.13	0.898
Sample Year (2017)					
2018	-0.15	0.47	519.08	-0.33	0.745
2019	-0.85	0.54	423.70	-1.57	0.116
2020	-0.80	0.55	380.92	-1.46	0.145
2021	-1.13	0.52	377.58	-2.20	0.029
2022	-0.56	0.49	363.36	-1.14	0.254

2023	-0.06	0.55	281.62	-0.11	0.916
Random					
Individual ID	1794 observations	89 individuals	Variance	0.995	

1052



1053

1054

1055

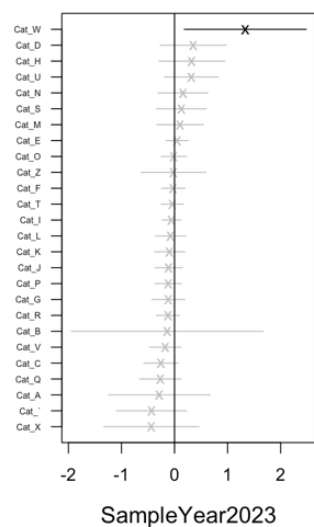
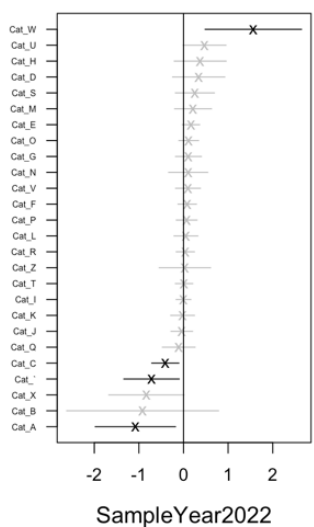
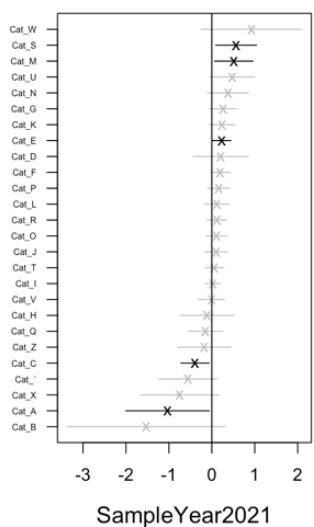
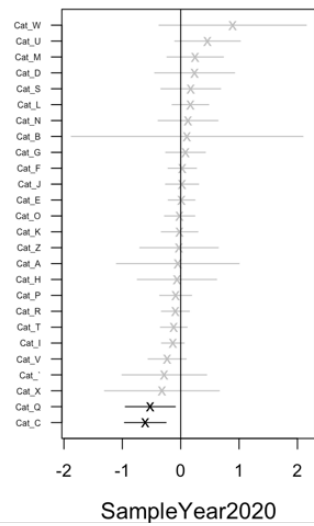
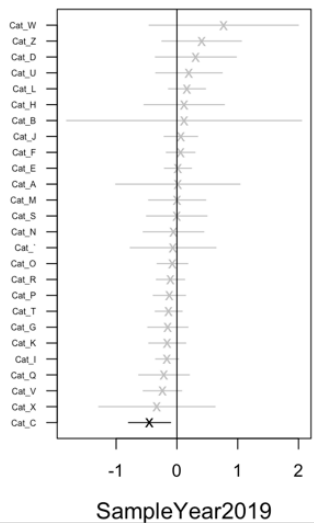
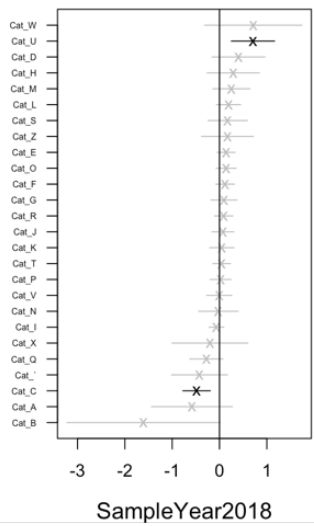
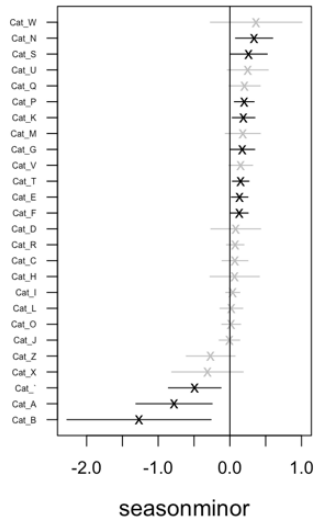
1056

1057

1058

1059

Figure S10. Differential abundance analysis of functional gut microbiome cluster of orthologous genes (COG) categories in Seychelles warblers using ANCOMBC2 with season and sample year. Each COG category is represented by a letter on the y-axis. Details of all COG categories are given in Table S5 [71]. "Cat_`" represents eggNOG annotations that were not assigned a COG category. Points and error bars are coloured according to significance (green: $p < 0.05$; grey: $p > 0.05$).



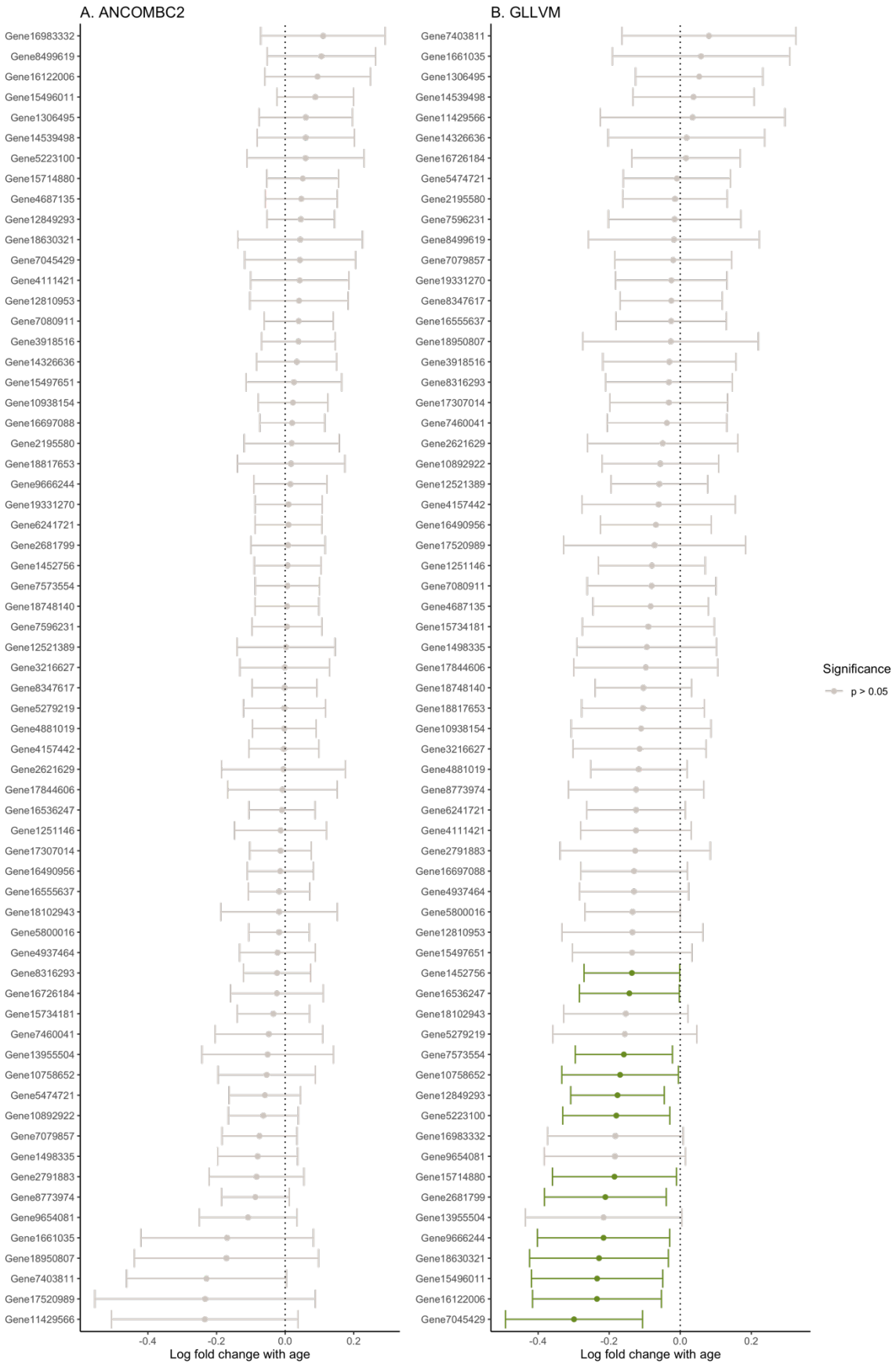
1060
1061
1062
1063

Figure S11. Differential abundance analysis of functional gut microbiome cluster of orthologous genes (COG) categories in Seychelles warblers using GLLVM with season and sample year. Each COG category is represented by a letter on the y-axis. Details of all

1064 COG categories are given in Table S5 [71]. "Cat_`" represents eggNOG annotations that
1065 were not assigned a COG category. Points and error bars are coloured according to
1066 significance (black: $p < 0.05$; grey: $p > 0.05$).

1067

1068



1069

1070

1071

Figure S12. Differential abundance analysis of functional gut microbiome COG2801 gene catalogue that were commonly (20% prevalence) found in Seychelles warblers using (A)

1072 ANCOMBC2 and (B) GLLVM. Each gene catalogue (95% average nucleotide identity) are
1073 represented on the y-axis by their gene catalogue number. Points and error bars are
1074 coloured according to significance (black: $p < 0.05$; grey: $p > 0.05$).

1075

1076